IEEE Access
Multidisciplinary | Rapid Review | Open Access Journal

Date of publication xxxx 00, 0000, date of current version xxxx 00, 0000.

Digital Object Identifier 10.1109/ACCESS.2017.DOI

Inverse Synthetic Aperture Radar Imaging: A Historical Perspective and State-of-the-Art Survey

RISTO VEHMAS[1] and NADAV NEUBERGER[2]
[1]Elettronica GmbH, Meckenheim, Germany (e-mail: r.vehmas@elettronica.de)
[2]Fraunhofer FHR, Wachtberg, Germany (e-mail: nadav.neuberger@fhr.fraunhofer.de)

Corresponding author: Risto Vehmas (e-mail: r.vehmas@elettronica.de).

ABSTRACT Radar can obtain high spatial resolution at large operating distances and its operation is largely independent from weather and lighting conditions. This makes it an important instrument in an ever-increasing number of applications requiring robust and reliable sensing of the environment. Due to the advancements in semiconductor technology and digital computation power, radar can obtain increasingly better position estimation accuracy, detection sensitivity, and target resolution. High-resolution imaging is an example of a rapidly advancing field of radar technology. Inverse synthetic aperture radar (ISAR) is an imaging technique that uses the motion of a target to obtain a high-resolution radar image of it. This paper presents a comprehensive review of past work and the state-of-the-art in ISAR imaging systems, algorithms, and applications. Starting from the early historical developments of simple monostatic range-Doppler imaging, we present the developments up to the current advanced spatially distributed imaging modalities and reconstruction algorithms. The list of references includes the most influential ISAR publications in the open literature up to early 2021.

INDEX TERMS Inverse synthetic aperture radar, radar imaging, radar signal processing, motion compensation, image reconstruction

I. INTRODUCTION

A. BACKGROUND

Radar has several benefits when compared to more traditional imaging sensors such as optical, infrared, or hyperspectral cameras. First, radar can provide a very high spatial resolution independent of the distance to the imaged target scene, since the resolution only depends on the bandwidth, wavelength, and possible relative movement between the radar and the target. Second, radar can operate independent from sunlight during day or night since it is an active sensor. Moreover, the electromagnetic waves at typical radar wavelengths can penetrate many visual obstacles such as clouds, fog, or smoke, making the image quality largely independent of weather conditions.

High-resolution radar imaging using the synthetic aperture principle is a powerful tool for a large number of surveillance and environmental monitoring applications [1]. Synthetic aperture radar (SAR) is an imaging technique based on using the motion of the radar platform to create a large synthetic antenna corresponding to a narrow beamwidth, i. e., a high angular (cross-range) resolution [1]–[3]. In SAR imaging, the radar typically collects the data while moving on board an air- or spaceborne platform and then focuses the data collected along the flight path to form a high-resolution range-cross-range image of the ground surface.

High resolution in range is easily obtained by using a suitable high-bandwidth waveform. To get a focused target image with high cross-range resolution, a very narrow antenna beam is required. At large operating ranges, the diameter of a real aperture antenna would have to be impractically large to achieve this. Thus, an alternative solution – the so-called synthetic aperture principle – has to be adopted. By allowing the relative position between the target scene and the radar to change as a function of time, the received signal can be processed as if it had been received by a large synthetic array (whose diameter is determined by the platform trajectory). This enables the creation of a very narrow antenna beam in cross-range by digital signal processing after the signals have been recorded.

To create the synthetic aperture, only a suitable relative

motion between the radar and target scene is required. Thus, either the radar platform or the target (or both of them) needs to move during the data collection. When the motion of a moving target (instead of just the radar w. r. t. the ground surface) is used to create the synthetic aperture, the imaging technique is called inverse synthetic aperture radar (ISAR). Depending on the sensor characteristics and the relative motion, the result of an ISAR system is a 1-, 2-, or 3-D description of the target's spatial electromagnetic reflectivity distribution.

The radar images obtained by ISAR systems are commonly used to recognize unknown detected targets when cooperative identification is not possible. Alternatively, ISAR can be used as an additional independent information source even when cooperative identification is used. Non-cooperative target recognition (NCTR) techniques are used in maritime, airspace, near-space, and overland surveillance applications to identify targets such as vessels, aircraft, ballistic missiles, satellites, and ground vehicles.

Compared to SAR, the applications of ISAR have been much more limited. The required signal processing algorithms in ISAR are often more complicated due to unknown target motion. Additionally, SAR can be used to image and monitor large areas with multiple targets, whereas ISAR is usually limited to imaging one target at a time.

From a historical perspective, military applications have been the driving force behind NCTR and the related ISAR techniques. However, an ever-increasing number of civilian applications is currently emerging. For example, ISAR has recently been used in automotive [4], [5] and space surveillance [6]–[8] use-cases. The trend of ISAR imaging technology is moving towards higher spatial resolution and more advanced imaging modalities utilizing spatially distributed systems.

B. PAPER SCOPE AND STRUCTURE

The purpose of this paper is to present a comprehensive review of past developments and the state-of-the-art in ISAR imaging. During recent years, specialized textbooks concerning general ISAR theory and applications have been published [9]–[12]. These references provide a detailed theoretical description and demonstrate several applications of ISAR imaging. This paper supplements these references by providing a more complete description of the historical developments of ISAR and a more extensive survey concerning the various research topics in the open literature. We focus on ISAR systems and algorithms, which aim to produce a radar image of the target. We do not cover techniques that use these images in a further application, such as NCTR (or automatic target recognition, ATR) and polarimetric ISAR.

We begin the article by introducing the basic ISAR terminology and a simple signal model in Section II. The presented material aids in understanding the significance of the various algorithms and concepts described in the later sections. Readers familiar with basic ISAR theory and terminology may skip this introductory section.

The early historical developments of ISAR imaging are reviewed in Section III. Starting from the first applications in range-Doppler imaging of the Moon and the planets, we survey the early applications up to the introduction of turntable ISAR and imaging of air targets in the early 1990s.

Section IV reviews the developments in monostatic ISAR processing algorithms from the mid-1990s until today. The conventional assumption of dividing the target motion into translation and rotation as well as various motion compensation methods are reviewed.

Since the early 2000s, spatially distributed (bi- and multistatic) ISAR systems and the related processing algorithms have been of great research interest. Section V reviews the seminal work in these areas. Important concepts and applications such as passive bistatic ISAR and 3-D interferometric ISAR (InISAR) are surveyed.

Section VI surveys important recent applications of ISAR imaging. Ground moving target imaging from space- and airborne platforms is one use-case receiving a great deal of interest [13]. Another emerging research topic is imaging non-rigid targets with rotating parts (such as drones and helicopters). Additionally, a number of space surveillance radars with ISAR imaging capabilities have been developed recently.

The advances in computer science and signal processing can also be seen in the current trends of ISAR research. Section VII reviews the most recent algorithmic developments in ISAR, focusing on compressed sensing (CS) and machine learning (ML) techniques.

Finally, Section VIII concludes the paper and outlines the future trends in ISAR research and applications.

II. BASIC PRINCIPLES OF ISAR

A. BASIC DEFINITIONS

The term ISAR is defined in the IEEE standard radar definitions as [14]

> "An imaging radar in which cross-range resolution (angular resolution) of a target (such as a ship, aircraft, or other reflecting object) is obtained by a synthetic aperture formed by the rotation or translation of the target, as opposed to motion of the radar. Cross-range resolution of target whose exact angular motion is unknown (e. g. non-cooperative targets such as ships at sea) is often achieved by resolving in the Doppler domain the different Doppler frequencies produced by echoes from the individual parts of the object."

The basic ISAR operating principle for a monostatic system can be summarized as follows. First, the radar transmits a sequence of electromagnetic signals – in the form of a suitable high-bandwidth waveform – towards the imaged target. Commonly used waveforms include a pulsed linear frequency modulation (LFM), the stepped frequency waveform, or frequency modulated continuous wave (FMCW). Then, the radar receiver records the echoes from the target that are

This article has been accepted for publication in a future issue of this journal, but has not been fully edited. Content may change prior to final publication. Citation information: DOI 10.1109/ACCESS.2021.3104799, IEEE Access

scattered towards the receiver. By performing range (fast-time) matched filtering (pulse compression) for the received signal, a series of high-resolution range profiles is obtained as a function of slow-time t (or pulse number m). Slow-time is the time variable that remains constant during the formation of a single range profile and increases from one range profile to the next. In ISAR processing, the target is commonly modeled as a superposition of isolated and isotropic point scatterers (Born approximation).

Figure 1 illustrates the basic ISAR geometry for a monostatic setup where the imaged target is constrained to move on a 2-D plane. The primed coordinate system – whose origin is assumed to be located in the target's center of mass – is rigidly attached to the target. The spatial degrees of freedom for each instant of slow-time include the line of sight vector $\boldsymbol{r}_0$, i. e., the location of target's center, and the orientation of the primed coordinate system. The orientation is determined by the angle between the target velocity vector $\boldsymbol{v}$ and the line of sight vector $\boldsymbol{r}_0$. For simplicity, here we assume the target always to be oriented along $\boldsymbol{v}$. Importantly, the target aspect angle θ changes as the object moves in a suitable manner. Consequently, the range $R_p(t) = ||\boldsymbol{R}_p(t)||$ of every spatial position on the target and changes in a unique way as a function of slow-time. This creates the different Doppler frequencies for each scatterer required to resolve them in cross-range.

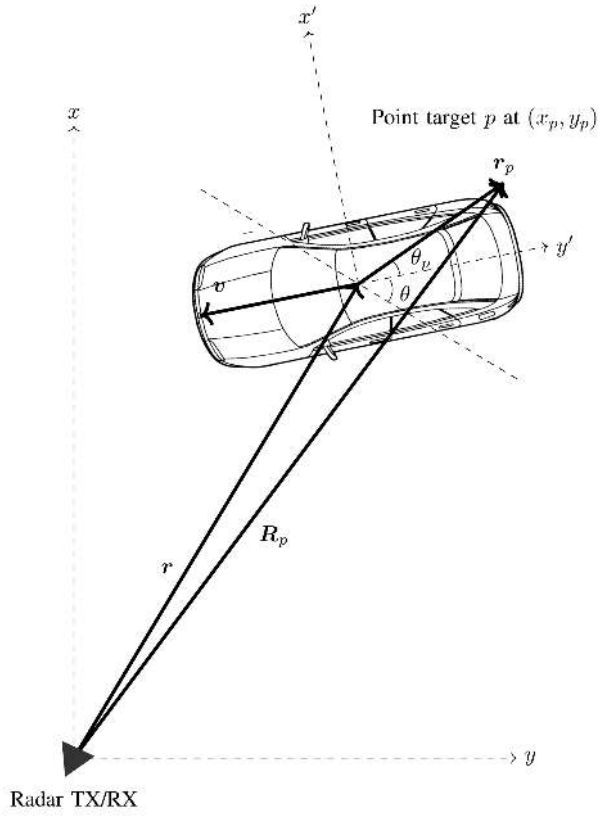

FIGURE 1. Illustration of the conventional monostatic 2-D ISAR imaging geometry. The change in the length of the line-of-sight vector $\boldsymbol{r}_0$ is called translational motion, whereas the rotational motion is defined as the change of the target aspect angle θ.

B. SIGNAL MODEL

In practical ISAR scenarios, the targets are objects such as cars, ships, satellites, or aircraft. The distance between the radar and the target is usually several kilometers, whereas the dimensions of the targets are much smaller. Thus, we can make a far field approximation $\|\boldsymbol{r}_0\| = r_0 \gg \|\boldsymbol{r}_p\| = r_p$. This can be used to derive an expression for the distance R_p between an arbitrary point on the object and the radar as [15]

$$R_p(t) \approx r_0(t) + x_p \cos\theta(t) + y_p \sin\theta(t), \tag{1}$$

where $x_p = r_p \sin\theta_p$ and $y_p = r_p \cos\theta_p$. This is a key result, because the motion can be divided into two parts: translation and rotation. The translation $r_0(t)$ is the same for every target point p (spatially invariant). Thus, it is not useful for ISAR imaging, since it gives each scatterer the same term in the Doppler frequency

$$f_p(t) = \frac{2}{\lambda}\frac{dR_p(t)}{dt} = \frac{2}{\lambda}\left(\frac{dr_0(t)}{dt} - x_p \sin\theta(t)\frac{d\theta(t)}{dt} + y_p \cos\theta(t)\frac{d\theta(t)}{dt}\right), \tag{2}$$

where λ is the carrier wavelength. The rotational motion $\theta(t)$ produces the unique (spatially variant) Doppler frequencies for different target points p required for obtaining the cross-range resolution.

In both SAR and ISAR, the so-called start-stop approximation is commonly employed. It means that we assume the target to be stationary during the formation of a single range profile. Assuming that the radar is illuminating a single point target at (x_p, y_p), the range profile can be expressed mathematically as

$$s_p(r,t) = a\left[\frac{2B}{c}(r - R_p(t))\right]\sqrt{\sigma(x_p,y_p)}e^{-i\frac{4\pi}{\lambda}R_p(t)}, \tag{3}$$

where B is the frequency bandwidth of the signal, c is the speed of light, and σ is the radar cross section (RCS) distribution of the target. Furthermore, a is the waveform's autocorrelation function. For example, in case of LFM we have $a(r) = \mathrm{sinc}(r)$. Using the Born approximation, we can write the reflectivity function of the target as a sum of P point scatterers as

$$g(x,y) = \sum_{p=0}^{P-1}\delta(x - x_p, y - y_p)\sqrt{\sigma(x,y)}, \tag{4}$$

where δ is the Dirac delta function.

As the target moves as a function of t, the distance R_p of each scatterer changes. Furthermore, the range profile of the target reflection can be expressed as a convolution between the point target response (3) and the target reflectivity function g. Mathematically, the ISAR signal model can thus be expressed as

$$s(r,t) = \Pi\left(\frac{t}{T}\right)\iint_{-\infty}^{\infty} g(x,y)s_p(r,t)dxdy, \tag{5}$$

This article has been accepted for publication in a future issue of this journal, but has not been fully edited. Content may change prior to final publication. Citation information: DOI 10.1109/ACCESS.2021.3104799, IEEE Access

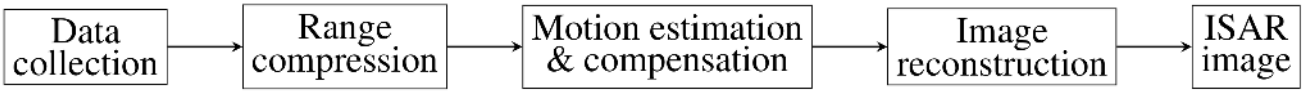

FIGURE 2. Flow-chart depicting the conventional ISAR processing chain. Target motion estimation and compensation are prerequisites for successful image reconstruction.

where Π is the rectangle function and T is the length of the coherent processing interval (CPI).

It is helpful to consider the signal model in the range spatial frequency k_r domain by taking the Fourier transform of (5) w. r. t. the range variable r. Assuming that $a(r) = \mathrm{sinc}(r)$, using the convolution theorem, and plugging in R_p from (1) we get

$$S(k_r, t) = e^{-i2(k_r+k_c)r_0(t)} \Pi\left(\frac{t}{T}\right) \Pi\left(\frac{k_r c}{2\pi B}\right) \times G(2k_r \cos\theta(t), 2k_r \sin\theta(t)), \tag{6}$$

where $k_c = (2\pi)/\lambda$ and $G(k_x, k_y)$ is the two-dimensional Fourier transform of the reflectivity function g.

The expression in (6) is a key result for both ISAR and spotlight mode SAR [3], [16]. It can be interpreted as follows: The range-compressed radar signal is a series of phase-modulated slices of the 2-D Fourier transform of the reflectivity function g. The rectangle function in (6) represents the fact that the signal is band-limited in k_r (which is an approximation, since the range profile is assumed to be of finite support). Consequently, the slices span an annulus sector in the 2-D spatial frequency domain. To successfully reconstruct the target image g, we need to compensate the phase modulation caused by r_0 and know the angles $\theta(t)$ to calculate the inverse Fourier transform.

In non-cooperative ISAR, the difficulty arises from the fact that both r_0 and θ are unknown *a priori*. To reconstruct a properly focused image, their values as a function of slow-time have to be somehow estimated. It is also evident from (6) that r_0 is a nuisance that does not provide any useful information for the image reconstruction. Its estimation is referred to as translational motion compensation. Correspondingly, the estimation of θ is referred to as rotational motion compensation.

C. IMAGE RECONSTRUCTION AND MOTION ESTIMATION

The results in (5)–(6) aid understanding the ISAR image reconstruction process. The problem is to estimate the spatial reflectivity distribution $g(x, y)$ given the received signal (5). Essentially, we need to apply a slow time-dependent matched filter h for each image position to recover g. Mathematically, this can be expressed as

$$I(x, y) = \iint_{-\infty}^{\infty} h^*(r, t; x, y) s(r, t) dr dt, \tag{7}$$

where I denotes the ISAR image. Ideally, the filter h is the impulse response of a point target located at position (x, y). Thus, the phase behavior of h is determined by the relative motion (r_0 and θ). For non-cooperative targets, a prerequisite for calculating (7) is target motion estimation. Since the matched filtering is based on coherently combining the range profiles, the motion has to be estimated very precisely (within a fraction of the wavelength λ) to obtain well-focused images. In SAR imaging, very accurate information about the relative motion is usually provided by a global positioning system (GPS) and inertial sensors. However, since in non-cooperative ISAR the target motion is unknown and unpredictable, the estimation problem is much more difficult.

In the 2-D model described above, we have two degrees of freedom (r_0 and θ) for each instant of slow-time. In case the target moves in 3-D, additional degrees of freedom need to be introduced. In general, these are two additional angles that describe the orientation of the primed coordinate frame (now including a third coordinate z') in the unprimed frame. Because the number of range profiles M is typically in the order of hundreds, the total number of unknown degrees of freedom $2M$ is often prohibitively large to allow a computationally feasible solution.

Thus, many assumptions and approximations have to be made in order to successfully estimate the target motion. These are application-dependent, and no successful general method to solve the motion estimation problem has thus far been presented. This has led to a large number of different motion compensation and image reconstruction algorithms in the ISAR literature. The different methods contain various trade-offs between estimation accuracy (robustness), image resolution (information content), computational requirements, and system complexity.

The simplest approach to ISAR is the so-called range-Doppler (RD) algorithm, where the Fourier transform is used as the matched filter for each range bin of the signal (5). However, this method is not often applicable to high-resolution imaging, since it requires many assumptions to be satisfied. First, the range R_p of each scatterer should not change more than the range resolution $\Delta r = c/(2B)$ during the CPI. Otherwise, scatterers migrate from one range bin to another causing smearing in range and a reduced Doppler resolution. Moreover, for the Doppler frequency f_p (see (2)) of each scatterer to be constant, we need to make a small angle approximation and the aspect angle needs to change linearly.

Whereas the RD technique represents the most simple and crude reconstruction method, back-projection (BP) is the most accurate and general way to reconstruct the image. In BP, the point target response (4) is used as the matched filter

This article has been accepted for publication in a future issue of this journal, but has not been fully edited. Content may change prior to final publication. Citation information: DOI 10.1109/ACCESS.2021.3104799, IEEE Access

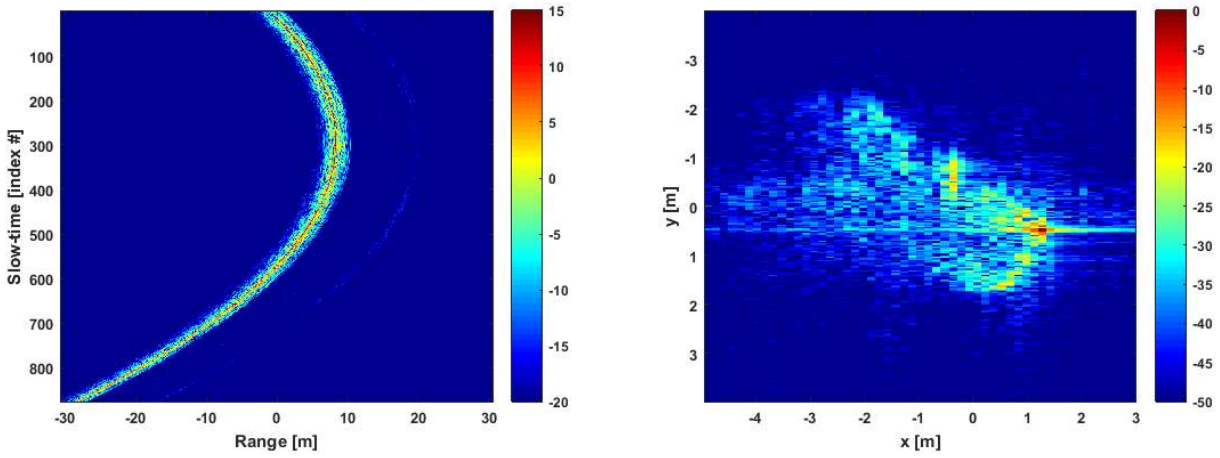

FIGURE 3. The intensity of the range-compressed data before ISAR processing (left) and the reconstructed ISAR image of the target passenger car (right).

h for each image position (x, y). The difficulty in using BP lies in the fact that the motion parameters r_0 and θ need to be known a priori to construct the matched filter h. Moreover, calculating the 2-D correlation integral (7) for each image pixel position (x, y) is computationally very intensive. This makes it very difficult to incorporate a motion estimation approach with BP.

The flow-chart of Figure 2 summarizes the typical steps required to obtain ISAR images described in this section. The model in (5) represents the signal after range compression. For clarity, the flow-chart depicts motion compensation and image reconstruction as separate steps. However, in some cases they are performed jointly and it is not possible to distinguish them into separate processing steps.

Figure 3 presents an example of actual X-band ISAR data of a passanger car. The plot on the left shows signal intensity after range compression (range profiles). The movement of the car during the CPI manifests itself as the changing location of the intensity distribution inside the range gate. The plot on the right shows the reconstructed ISAR image with a spatial resolution of approximately 15 cm. In this example, the radar and the car are located on the same ground plane. For this reason, the car corner closest to the radar produces the strongest reflection whereas the opposite corner is shadowed.

D. SPATIALLY DISTRIBUTED SYSTEMS

Bi- and multisatic ISAR systems have spatially separated transmitter(s) and receiver(s). This setup can be used to obtain 3-D images of targets, more useful information about the target reflectivity, and more degrees of freedom for the motion estimation. Moreover, they can be used as passive ISAR sensors. Importantly, spatially distributed ISAR is more robust against unfortunate imaging geometries – for a monostatic sensor, a radially moving target is impossible to resolve in cross-range (since the Doppler shift of each scatterer is the same).

Even though the above-described signal model only holds for a monostatic geometry, the basic concepts are essentially the same for the spatially distributed case. A detailed analysis of the spatially distributed ISAR signal model is outside the scope of this paper. References [17], [18] provide a detailed description of the bi- and multistatic ISAR models, respectively. Spatially distributed ISAR methods are surveyed and analyzed in more detail in Section V of this paper.

III. EARLY HISTORICAL DEVELOPMENTS

We begin our survey by providing a historical perspective for ISAR imaging. This section surveys the early ISAR developments from the late 1950s up to the early 1990s. The important early milestones illustrated in the timeline of Figure 4 are described next.

A. RADAR ASTRONOMY

The seminal paper by Ausherman *et al.* [19] summarizes the ISAR earliest developments concisely. The concept was formulated for the first time in the 1950s in the context of radar astronomy [20] with the aim of improving the resolution of the radars measuring the surfaces of the Moon and the planets of the Solar system. In these cases, the rotation of the planets and the Moon was used to obtain the differential Doppler resolution capability [21]–[23], though the term ISAR was introduced only later by the radar community.

The first radar images of the Moon were obtained by the Millstone Hill radar, operating at 440 MHz center frequency [24]. The images had a range resolution of 75 km and a Doppler resolution of 0.1 Hz, obtained from a CPI of 10 seconds. During the following years, the same concept was used to obtain images of different planets. The Millstone radar was used to acquire images of Venus and Mercury [25]–[27]. The Arecibo telecscope was used to measure and analyze the Doppler spectrum of Mercury, Mars, and Jupiter [28]–[31]. However, the Arecibo instrument was not able to properly resolve the planets in range due to its low-bandwidth waveform. Thus, the Doppler spectra were used to estimate

This article has been accepted for publication in a future issue of this journal, but has not been fully edited. Content may change prior to final publication. Citation information: DOI 10.1109/ACCESS.2021.3104799, IEEE Access

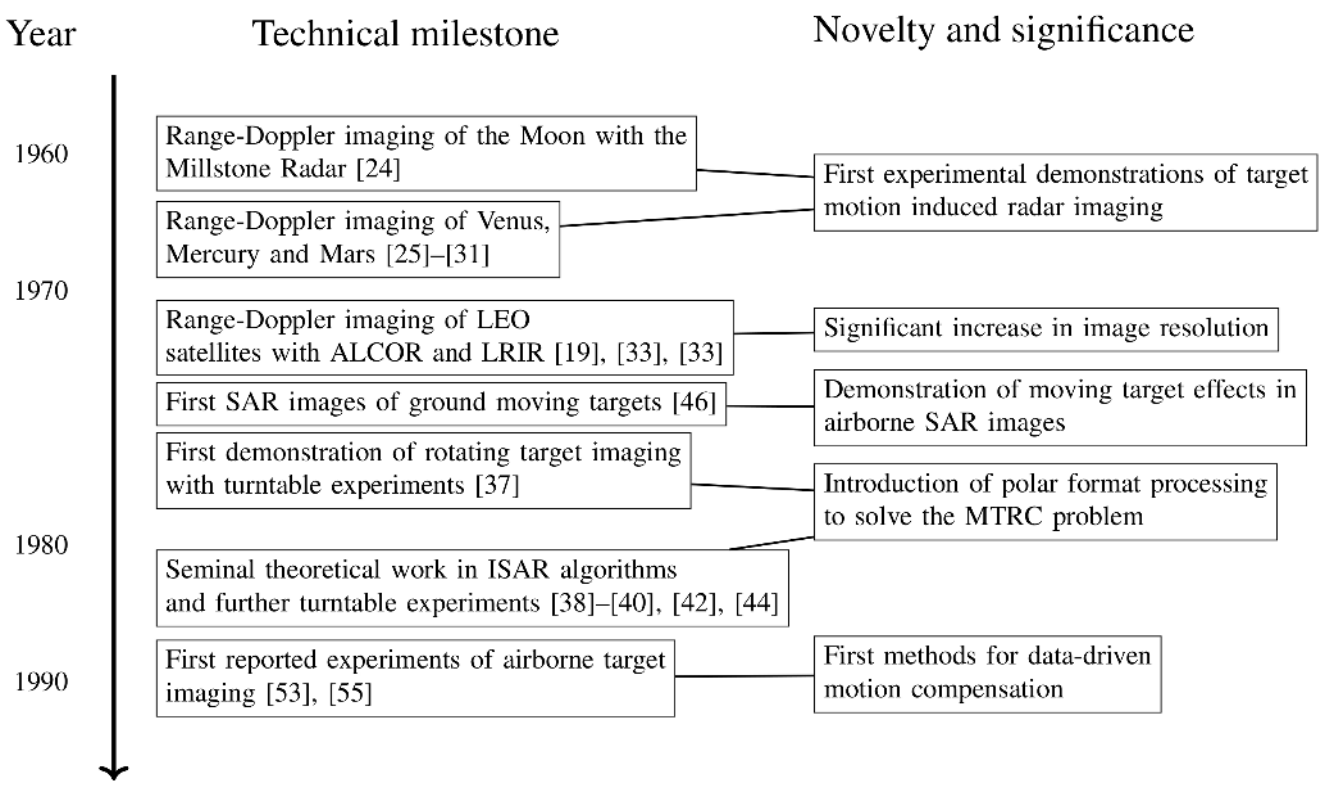

FIGURE 4. Timeline of early historical developments of ISAR imaging systems, algorithms, and applications.

the planets' rotation parameters, not to map their surfaces. Nevertheless, the Doppler analysis technique used in this case was essentially based on the ISAR principle.

B. SPACE TARGET IMAGING

The next significant developments occurred in the late 1960s when it was recognized that the range-Doppler technique could be applied to imaging of satellites orbiting the Earth in space. For the purpose of space target identification, a radar operating at 94 GHz with a bandwidth of 1 GHz using LFM was developed by the Aerospace Corporation [32]. The first radar images of space targets were obtained by the Advanced Research Projects Agency (ARPA) Lincoln C-band Observables Radar (ALCOR) in the early 1970s [33]. The range resolution of ALCOR was initially 50 cm, and the system was later developed – due to the success of early ALCOR results – to have a higher pulse repetition frequency (PRF) and more robust data acquisition for imaging purposes [19], [33].

In the 1970s, the next significant advancement in this field was the development of the long-range imaging radar (LRIR) by the Lincoln Laboratory [34]. LRIR had a range resolution of 25 cm and a PRF of 1000 Hz at X-band, allowing high quality imaging of rapidly rotating space targets. In this context, significant progress was also made in the signal processing algorithms used to reconstruct the target images, leading to increased spatial resolution. Concepts for using longer CPIs were developed to achieve wide-angle an 3-D imaging capabilities [19], [34].

C. TURNTABLE IMAGING

The first developments for imaging rotating ground-based targets began in the 1960s at the Willow Run Laboratories. It was recognized that the concept was essentially equivalent to SAR imaging, which had been introduced during the previous decade [35]. The first experiments were carried out using a rotating platform (turntable) and a coherent ground-based radar system. The turntable setup provided a well-controlled environment allowing the development and demonstration of increasingly advanced imaging algorithms. Initially, the image reconstruction was based on using the Fourier transform and a simple procedure to compensate for the scatterer migration through range resolution cells (MTRC) [36].

A more general formulation of the rotating target imaging problem was given by Walker [37], [38]. He introduced the polar format data storage and processing concept, which solved the scatterer MTRC problem. MTRC occurs when the scatterer ranges R_p change more than the range resolution Δr during the CPI, which is common in high-range resolution and wide-angle imaging. The algorithms and the results of the turntable experiments were reported in the seminal paper [38]. Early theoretical developments of ISAR were also reported in [39], [40]. At about the same time, Mensa *et al.* [41], [42], Wehner *et al.* [43], and Chen *et al.* [44], [45] also reported their first concepts and results in range-Doppler imaging of rotating targets.

This article has been accepted for publication in a future issue of this journal, but has not been fully edited. Content may change prior to final publication. Citation information: DOI 10.1109/ACCESS.2021.3104799, IEEE Access

D. OTHER EARLY DEVELOPMENTS

In the early 1970s, Raney demonstrated imaging ground moving targets using an airborne SAR system [46]. The concept was further developed and demonstrated in the 1980s [47], [48] and early 1990s [49]–[51], and also applied to imaging maritime targets [52]. The motion estimation and compensation of the non-cooperative targets was achieved by using the dominant scatterer technique (i.e., estimating the phase of prominent point scatterers on the target as a function of slow-time) [2], [49] or by using time-frequency analysis techniques [50], [51].

In the late 1980s, first results from imaging airborne targets with ground-based ISAR systems were reported. Steinberg [53] presented X-band images of an aircraft with one meter resolution. First concepts related to estimating the target motion without *a priori* knowledge were also presented for this purpose [54], [55]. They were also based on estimating the phase of multiple dominant scatterers on the target.

Since the mid-1990s, the number of reported applications for ISAR has steadily increased with a trend towards increased spatial resolution and more sophisticated imaging modalities. The earliest applications of imaging ground-based moving targets from air- or spaceborne platforms as well as imaging space targets at the low Earth orbit (LEO) region remain very active application and research areas. This is due to the need for active space surveillance to prevent space debris collisions with active satelites [8]. Modern applications and developments in these areas are reviewed in more detail in Section VI. The important later developments described in the next sections are summarized in the timeline of Figure 5.

IV. MONOSTATIC ISAR PROCESSING

Following the developments described in the previous section, the motion compensation and image reconstruction algorithms required for successful ISAR imaging have received a great deal of interest in the open literature. Up to the early 2000s, most of the systems and methods were developed in the context of monostatic ISAR – e. g., all of the early systems described in the previous section are monostatic. This section reviews the various ISAR motion compensation and image reconstruction algorithms that have been developed and demonstrated for monostatic ISAR systems. It should be noted that many of these methods can be used for bi- and multistatic processing as well – albeit usually with some modifications.

Instead of going through the developments in chronological order, we review specific problems and the methods used to solve them in a sequential manner. Each of the next two subsections deals with a distinct aspect of the ISAR processing. In Section IV-A, we first consider the methods to estimate and compensate the translation r_0 of the target. Then, we proceed to review the approaches used for estimating the target rotation θ and performing the image reconstruction in Section IV-B.

A. TRANSLATIONAL MOTION COMPENSATION

Translational motion compensation is commonly divided into two parts. The first part performs an initial coarse estimation and is called range alignment. It aims to compensate the target translation to an accuracy comparable to the range resolution Δr, i. e., to "align" the range profiles. It first estimates $r_0(t)$ and then shifts the range profiles to compensate for the changing range. The second part called autofocus performs a fine estimation to accurately remove the residual spatially invariant phase errors remaining after range alignment.

The division into two steps is usually done due to computational reasons. However, it is also possible to estimate and compensate the translation using a single-step approach. Figure 6 summarizes these two classes of different methods for translational motion compensation. Next, we review the specific techniques in more detail.

Range Alignment

The first and simplest range alignment method was based on choosing a reference range profile (usually corresponding to the first pulse of the CPI) and calculating the cross-correlation between it and the other range profiles to determine the range shifts [53], [56]–[58]. However, the accuracy of this method suffers if the target reflectivity distribution (RCS) changes during the CPI due to rotation. A way to avoid this problem is to correlate each adjacent range profile (and thus estimate the differential range shifts). However, this method is vulnerable to error accumulation, since the final estimation is obtained by integrating the estimated differential range shifts. More recently, extensions to the cross-correlation method have been developed to partially overcome the above-mentioned problems [59], [60].

Methods based on the Hough transform [61] and keystone formatting [62]–[65] have also been successfully used for range alignment. Of these two methods, keystone formatting also plays an important role in rotational motion compensation, as described later. Both of these methods assume a simple model (first or second order polynomial) for r_0 as a function of slow-time. Keystone formatting is based on eliminating the range-Doppler coupling by a re-scaling of the slow-time variable in the (k_r, t) domain. The Hough transform is a well-known method that can be used to find specific shapes in images. In this case, it is used to find the first or second order curves traced by the target in the range-compressed (r, t) domain.

Several other range alignment methods are based on optimizing a quality measure calculated from the amplitude of the range profiles. The minimum entropy method [66]–[68] is based on minimizing the entropy of the sum of two adjacent profiles as a function of the range shift applied to one of the profiles. The global range alignment method [69], [70] estimates the translation by minimizing a loss function, whose value quantitatively measure the quality of the range alignment for the entire CPI. Several different quality measures have been proposed [71], [72], such as the

This article has been accepted for publication in a future issue of this journal, but has not been fully edited. Content may change prior to final publication. Citation information: DOI 10.1109/ACCESS.2021.3104799, IEEE Access

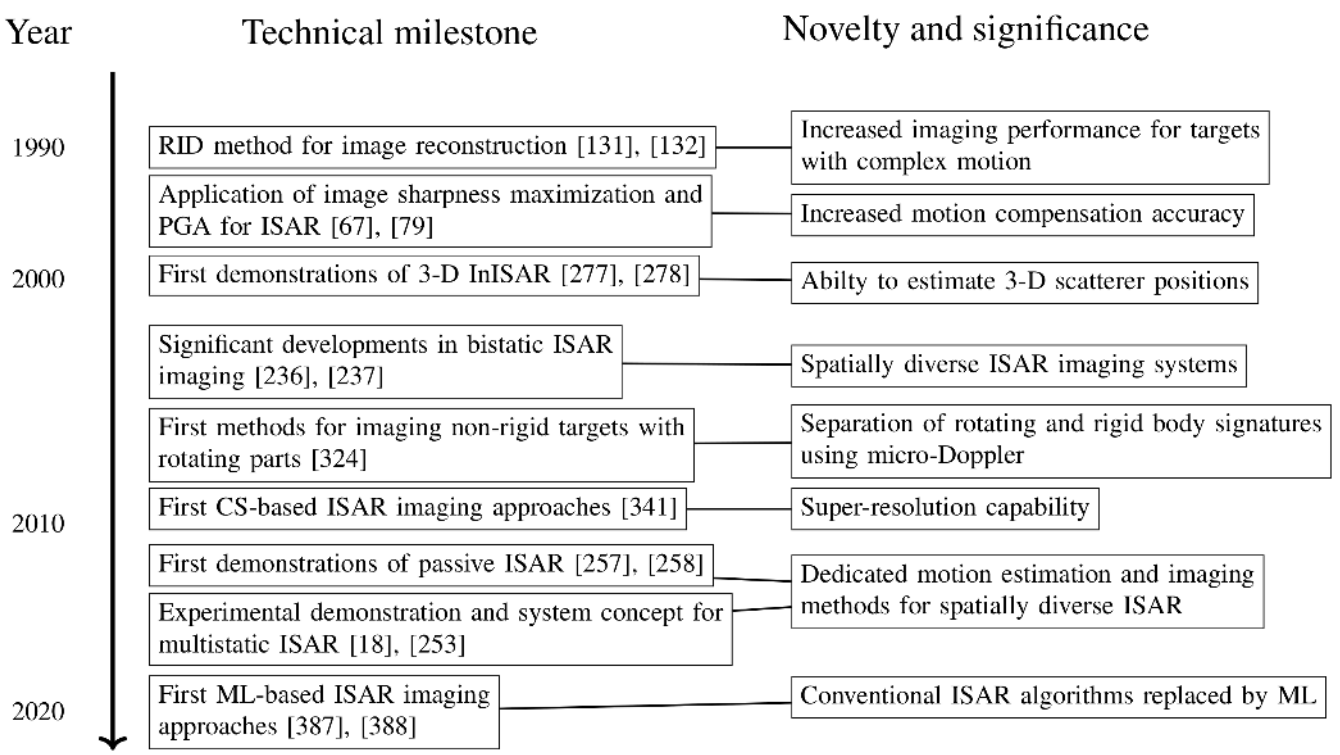

FIGURE 5. Timeline of later significant developments of ISAR imaging systems, algorithms, and applications.

contrast and entropy of the average range profile and the sum of the squared differences of adjacent range profiles.

The global method uses the entire CPI to estimate the motion, whereas the minimum entropy method operates on a pulse-to-pulse basis. A disadvantage of the global method is an increased computational complexity, which means that usually a parametric model needs to be used for $r_0(t)$. The minimum entropy method is essentially non-parametric. Methods to speed up the computation of the global method have been proposed in [72], [73]. An efficient hybrid between the global and local pulse-to-pulse methods uses the average range profile (i. e., data from the entire CPI) in the loss function but does the estimation on a pulse-to-pulse basis [74]–[76]. This method is more robust when the target exhibits rapid motions not easily captured by a low-order parametric model.

Currently, the most important limitations of range alignment methods are related to poor performance under low signal-to-noise ratio (SNR) and sensitivity to significant changes of the target RCS during the CPI. The optimization-based approaches suffer the most in the presence of low SNR, because the quality metrics only use the absolute value of the range-compressed signal – i. e., a possible coherent integration gain is not utilized. An underlying basic assumption behind all of the methods is that the target RCS is constant during the CPI. In practice, this means that the target should not rotate much during the CPI. The global method provides the most robustness against target rotation, whereas the cross-correlation method is the most sensitive to it. Table 1 summarizes the most important strengths and weaknesses of the range alignment methods described above.

Autofocus

After range alignment is performed, a slow-time-dependent phase error motion may remain in the data. This is because range alignment is essentially a non-coherent procedure: It only takes into account the amplitude envelopes of the signal. Moreover, some sources of phase errors (e. g., target vibrations or atmospheric distortions) may be so small that they do not cause a noticeable range shift while still significantly distorting the slow-time phase – necessitating an additional phase compensation step.

In the SAR (and ISAR) literature, autofocus refers to the residual translational motion compensation that is applied to each range bin signal after range alignment. It has been extensively studied in the the context of airborne spotlight mode SAR [2], [3] and synthetic aperture sonar imaging [77], since the problem is essentially the same as in ISAR. Two well-known classes of autofocus algorithms are based on image sharpness maximization (a general term, which includes contrast optimization and entropy minimization) [67], [78]–[82] and phase gradient autofocus (PGA) [83], [84].

In sharpness maximization autofocus, the objective function is calculated from the image intensities: It can be e. g. the coefficient of variation of the image intensities or amplitudes [79], the sum of the squared intensities [82], or the entropy of the intensity image [67]. The sharpness maximization

This article has been accepted for publication in a future issue of this journal, but has not been fully edited. Content may change prior to final publication. Citation information: DOI 10.1109/ACCESS.2021.3104799, IEEE Access

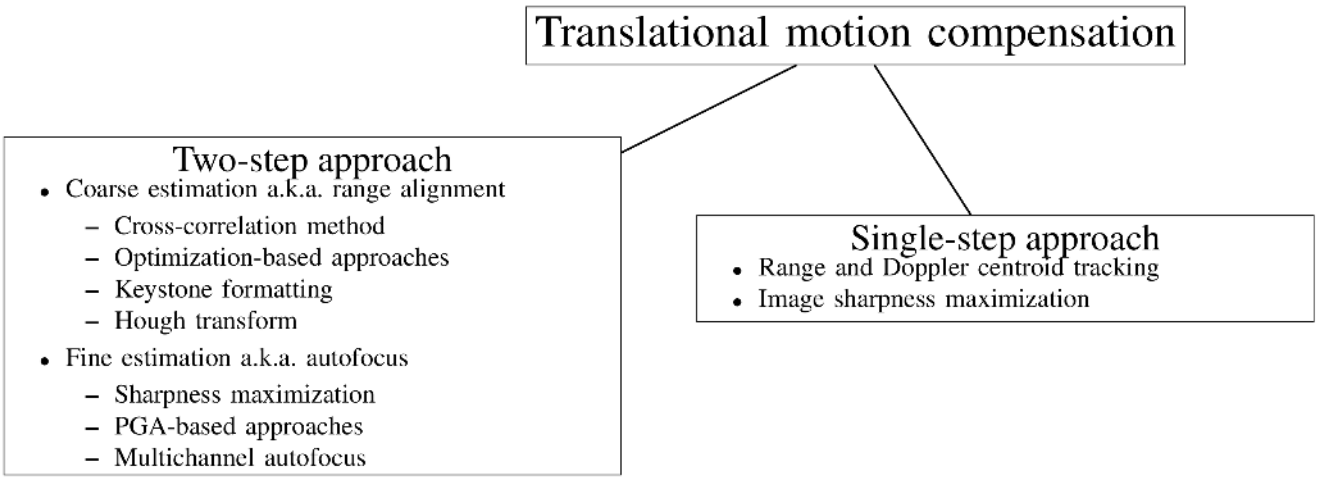

FIGURE 6. Methods used for translational motion compensation in conventional monostatic ISAR imaging. The two-step approach is computationally more tractable, but starts to break down for long CPIs with significant target rotation.

TABLE 1. Advantages and disadvantages of different range alignment algorithms.

Method	Advantages	Disadvantages
Cross-correlation method	Computatinally efficient No adjustable parameters	Error accumulation may occur Sensitive to RCS changes during the CPI
Optimization-based methods (e. g. global range alignment)	Most robust against RCS changes Information from the entire CPI is used	High computational cost Multiple adjustable parameters are needed Poor performance under low SNR
Keystone formatting	Computatinally efficient Insensitive to SNR Insensitive to RCS changes	Limited to a specific polynomial order for r_0
Hough transform	Computatinally efficient Relatively robust against RCS changes	Limited to a low-order model for r_0 Sensitive to SNR

autofocus can be considered as a local optimization problem [80]–[82]. Thus, it can be solved efficiently by first or second order local optimization algorithms [15], [82], [85]. Since the required numerical optimization is generally a computationally intensive task, several approaches have been proposed to improve the efficiency [15], [75], [85]–[93]. One option is to use a parametric model for the phase errors as a function of slow-time. Additionally, different image sharpness metrics have been analyzed and compared in references [94]–[96].

PGA uses an iterative procedure to estimate the unknown phase error [3], [84]. After isolating dominant scatterers in the image (range-cross-range) domain, the signal is transformed back into the range-slow-time domain to perform the phase error estimation. The process is repeated iteratively, since it becomes easier to isolate the point scatterers when the image focus increases. PGA is computationally more efficient than sharpness maximization. The conventional PGA [84] was limited to Fourier transform-based image reconstruction using a single strong scatterer per range bin for estimation. Due to this reason, extensions to PGA have been considered since its conception in the 1990s. More accurate and robust estimators have been proposed in [97]–[105]. The most recent advances [106], [107] propose an extension of PGA to allow its application for diverse imaging geometries and different image reconstruction methods.

Another well-established autofocus method called multichannel autofocus is based on a linear algebraic formulation of the phase error estimation problem [108]–[110]. It uses an assumption that the image support is limited (when the image is correctly focused, there is a region of approximately zero intensity pixels) to estimate the phase errors. The above-mentioned references have demonstrated its superior focusing performance compared to PGA and sharpness maximization for spotlight mode SAR images.

Sharpness maximization works well when the ideally focused image has a high contrast, i. e., one or multiple strong scattering centers on a weak background. On the other hand, when the ideally focused image has a relatively uniform intensity distribution, sharpness maximization may produce erroneous results. In this case, PGA is usually more robust. Even though PGA relies isolating strong scatterers, it averages the estimation result from each range bin to obtain the final result. In most ISAR applications, the target can be considered as a sum of point-like reflections with weak background (clutter) reflections. Thus, both sharpness maximization and PGA are widely used solutions in ISAR. The relative strengths and weaknesses of the above-mentioned autofocus algorithms are summarized in Table 2.

This article has been accepted for publication in a future issue of this journal, but has not been fully edited. Content may change prior to final publication. Citation information: DOI 10.1109/ACCESS.2021.3104799, IEEE Access

TABLE 2. Advantages and disadvantages of different autofocus algorithms.

Method	Advantages	Disadvantages
PGA	Computatinally efficient Good performace even for low-contrast images	Limited to the RD reconstruction method
Sharpness maximization	Compatible with any image reconstruction method Good performance for high-contrast images	High computational cost Requires targets with dominant scatterers or high contrast features
Multichannel autofocus	Computatinally efficient Superior estimation performance	Requires a low-return area in the image domain Limited to the RD reconstruction method

Single-Step Compensation

The above-described two-step approach to translational motion compensation is commonly used due to its computational efficiency. However, it has some drawbacks. Most importantly, the autofocus approach requires successful range alignment (residual error has to be smaller than the range resolution). In case range alignment fails to compensate the translation adequately, autofocus cannot remedy the situation. Thus, the two-step approach is ultimately limited by the accuracy of the range alignment algorithm. As mentioned previously, long CPIs present a problem even for the most robust range alignment methods. Increased cross-range resolution requires a longer CPI (larger target rotation), limiting the applicability of the two-step approach in very high-resolution ISAR imaging.

To overcome these limitations, several methods requiring only a single step of translational motion estimation and compensation have been considered in the literature. An early example of such a method is the centroid tracking approach [111]. In this approach, the translation is compensated by tracking and making the target centroid (defined as the weighted average of target range and Doppler) constant as a function of range and slow-time. Another early method was based on optimizing a burst derivative quality measure, which describes the image sharpness [112], [113]. Compared to sharpness maximization autofocus, the advantage is that the image reconstruction does not have to be performed to evaluate the burst derivative metric.

The sharpness maximization concept can also been used as a single-step approach. In this case, the estimation is extended from the residual slow-time phase to the full translation r_0. The main drawback of this approach is the resulting computational intensity – the autofocus problem can be considered as a 1-D (cross-range) focusing problem, whereas now the focusing needs to be done in 2-D (range and cross-range). Berizzi *et al.* [79] optimized the coefficients of a parametric translation model using the image contrast – defined as the ratio between the standard deviation and the mean of image intensities – as the objective function. The same approach has since been succesfully used with different optimization algorithms, objective functions and target motion models [114]–[119].

An approach based on the CLEAN algorithm, which uses multiple independent scattering centers on the target to estimate the translation, has been proposed in [120]. More recently, the Doppler centroid estimation method has been extended (to include estimating the Doppler rate) in [121]. In [122], a method based on using an improved version of the cross-correlation range alignment method with phase-derived velocity estimates is used to perform the single-step compensation.

B. ROTATIONAL MOTION COMPENSATION

After the translation r_0 has been compensated, the target rotation θ needs to be estimated to properly perform the image reconstruction. The rotation determines the phase progression of the slow-time matched filter h. The process of estimating the unknown rotational motion and using it in the image reconstruction is generally more complicated than the translational motion compensation. Many different methods for performing the slow-time filtering and estimating the target rotation have been proposed in the ISAR literature.

The most common approach is to divide the problem into two distinct parts: the image reconstruction filter and cross-range scaling. The purpose of the first part is to design such a filter that the target reflections are properly compressed into point-like responses in ISAR image domain. Since the slow-time signal can be considered as a superposition of signals with slow-time varying Doppler frequencies f_p, methods from time-frequency signal processing are commonly used for this purpose.

However, the problem of the time-frequency filtering methods is that they only estimate the Doppler frequency of the scatterers. The Doppler frequency is directly proportional to the cross-range position, but there is an unknown scale factor depending on the aspect angle change (target rotation) during the CPI. Moreover, the direction of the target rotation determines the image projection plane. In case the target is not constrained to move rigidly on a 2-D plane (see Figure 1), knowing the projection plane is crucial for interpreting the image and estimating the size of the target.

Methods for obtaining an estimate for the rotational angle are called cross-range scaling, since the Doppler axis can be properly scaled into spatial cross-range units when the rotation is estimated. This step is crucial for image interpretation and exploitation in NCTR applications.

Figure 7 summarizes the methods used for the above-mentioned two steps (image reconstruction filters and cross-range scaling) into different classes. Next, we review these algorithms in more detail.

Range-Instantaneous-Doppler Image Reconstruction

The simplest way to perform the image reconstruction is to use a 1-D Fourier transform, i. e., to assume a constant f_p

This article has been accepted for publication in a future issue of this journal, but has not been fully edited. Content may change prior to final publication. Citation information: DOI 10.1109/ACCESS.2021.3104799, IEEE Access

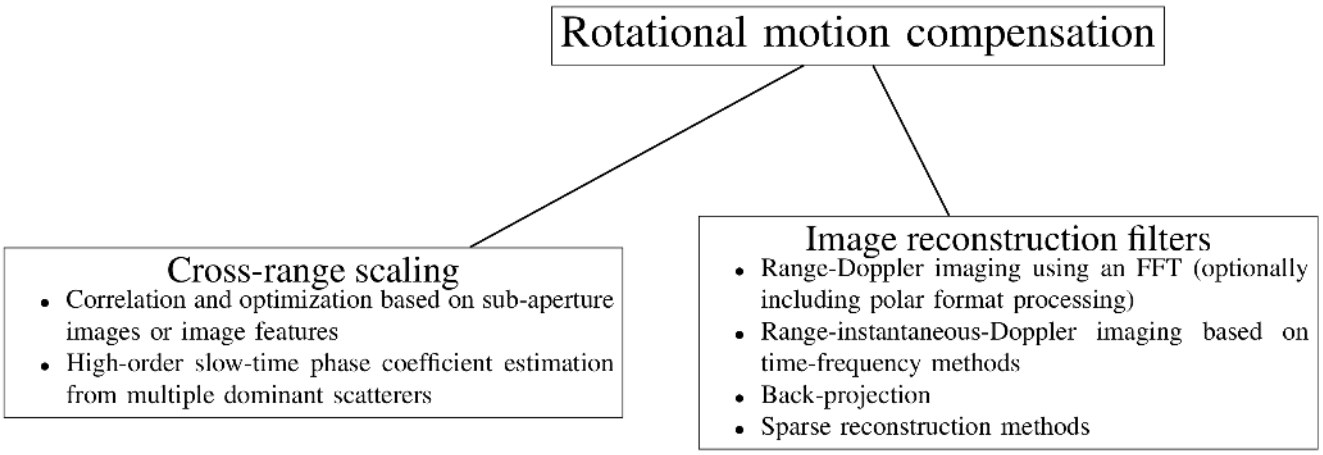

FIGURE 7. Methods used for rotational motion compensation in conventional monostatic ISAR imaging.

(linear slow-time phase progression) for each scatterer during the CPI. However, when the range resolution is extremely high and a similarly high resolution is desired in the cross-range direction, this simple RD algorithm rarely produces an acceptable result. As the CPI length and the rotational angle increase, scatterer MTRC and the time dependence of f_p cause defocusing and thus degraded image resolution (in both range and cross-range dimensions).

Moreover, if the rotational motion is not uniform, f_p is not constant even during a short slow-time interval. As a solution to the MTRC problem, a technique called keystone formatting can be used [15], [62]–[64], [123]–[130]. It was initially introduced by Perry *et al.* [62] in the context of airborne SAR imaging of moving objects. As previously mentioned, it can also be used to achieve range alignment. However, keystone formatting can only compensate for MTRC of a specific order. Commonly, either the linear or quadratic component is compensated.

To mitigate the effect of slow-time dependent scatterer Doppler frequencies $f_p(t)$ (non-linear phase histories), time–frequency representations (TFRs) can be used as the slow-time matched filter. This approach was first introduced by Chen [9], [131], [132] in the 1990s. Since then, it has matured into a well-established technique [133], [134] and many different TFRs have been successfully used in ISAR imaging. Theoretical analyses of various trade-offs in the TFR-based imaging approach – concerning metrics such as resolution and SNR – have been provided in references [133]–[137]. To distinguish this approach from the conventional Fourier transform-based RD algorithm, it is usually referred to as the range-instantaneous-Doppler (RID) method. The conventional RD approach uses the entire CPI to reconstruct a single ISAR image, whereas the RID approach produces a set of ISAR images (one for each slow-time instant) for the same CPI.

Variations of the Wigner-Ville TFR – trying to eliminate the harmful cross-terms inherent in it – have been succesfully used to reconstruct ISAR images in [138]–[142]. The so-called adaptive joint time-frequency (AJTF) transform [143] has also been demonstrated in a number of references [144]–[148]. Furthermore, the S-method [149] has been shown to greatly surpass the conventional RD approach in [15], [150]–[153]. The fractional and local polynomial Fourier transforms represent a compromise between the pure RD and RID methods: Instead of transforming the signal into the full slow-time-Doppler domain, they only calculate the TFR along a certain line (linear combination of t and f_p) in the TFR plane [154], [155].

More recently, such methods from time-frequency signal processing as the synchrosqueezing transformation [156] and time-frequency reassignment [157] have been demonstrated in ISAR applications [130], [158], [159]. These methods have the potential of even further improving the image focus and mitigating the effect of sidelobes in the image domain.

References [160]–[163] use the chirplet decomposition to perform the slow-time filtering. In these methods, the signal in each range bin is considered to be a superposition of "chirplets", which are basis functions $\exp i\phi(t)$ whose slow-time phase history $\phi(t)$ follows a chosen model (most commonly quadratic or cubic). A number of different methods based on this assumption (superposition of quadratic or cubic phase signals) has been developed and demonstrated more in references [164]–[185]. These methods are based on estimating the Doppler modulation parameters (second and third order phase coefficients), which can then be used to estimate the rotation and perform the slow-time filtering.

The large number of different RID methods demonstrates the difficulty of formulating a general method for ISAR imaging. Choosing a suitable method largely depends on *a priori* knowledge about the possible target types and their motion dynamics, RCS distributions, etc. The RID method is more robust and produces a better cross-range resolution than RD in cases where the target exhibits complex motions. However, this robustness comes at the cost of having to tune the parameters of a chosen TFR to a specific use-case, limiting general applicability. Moreover, the well-known time-

This article has been accepted for publication in a future issue of this journal, but has not been fully edited. Content may change prior to final publication. Citation information: DOI 10.1109/ACCESS.2021.3104799, IEEE Access

TABLE 3. Advantages and disadvantages of different ISAR image reconstruction filters.

Method	Advantages	Disadvantages
RID imaging using TFRs	Computationally efficient Easy to integrate with other motion compensation	TFRs contain many adjustable parameters Unavoidable trade-off between image resolution and TFR cross terms
BP	Non-approximated filtering method Easy implementation without adjustable parameters	High computational cost Difficult to integrate with motion compensation
Non-linear methods	Super-resolution capability Suppressed image sidelobes	High computational cost Difficult ot integrate with motion compensation Sensitive to noise

frequency uncertainty relation of TFRs also presents a performance limitation for RID imaging. In other words, a compromise between the CPI length, TFR cross-term suppression, and cross-range resolution is unavoidable in one form or another.

Other Methods

Even though the TFR-based RID approach mitigates the effects of non-linear slow-time phase histories (changing f_p), it is not a complete solution to the problem. To mitigate the above-mentioned limitations, a number of other rotation estimation and image reconstruction techniques have been proposed.

A general way to reconstruct the image without any approximations is the BP algorithm. However, it is computationally very intensive when combined with a data-driven motion estimation method (usually including numerical optimization). Thus, BP has so far been mostly limited to imaging of cooperative targets, where the target motion is known *a priori* [186]–[190].

More recently, BP algorithms with integrated motion compensation have been considered in [191], [192]. However, these methods require approximations concerning the target motion to be made to realize a computationally efficient implementation. The BP approach has had more success for a multistatic setup, where the motion estimation is easier due to the increased degrees of freedom provided by the spatial diversity [18]. This method is later described in Section V.

Several non-linear filtering methods have also been used in ISAR. The most popular approach is to use sparse reconstruction algorithms from CS. These methods, whose use has increased significantly during the recent years, are reviewed in Section VII-A. Other examples of applying non-linear slow-time filtering in ISAR include the Capon method [193], the iterative minimum means squares error (MMSE) method [194], the weighted least squares-based iterative adaptive approach [195], and super-resolution techniques [196]. These methods have been shown surpass the RD and RID methods in terms of image resolution in specific examples. However, the increased performance comes at a cost. The methods require a high SNR to work well, the target reflectivity often needs to follow a specific model, and the computational cost is high.

Table 3 summarizes the strengths and weaknesses of the different image reconstruction filters described above. Whereas the RID approach remains the most widely used concept due to its computational efficiency, BP and CS-based methods are becoming more attractive as the available computation power continues to increase.

Time Window Optimization

In a typical operational scenario, the radar measures the non-cooperative target as long as it remains in its field of view. This often results in a large amount of recorded data, and thus it becomes necessary to choose a suitable subset (CPI) to perform the ISAR imaging. If the CPI is too short (and the target barely rotates during it), motion compensation is easy but the cross-range resolution will be poor. When the CPI is long and the target rotates significantly during it, high cross-range resolution can be obtained. However, motion compensation becomes more difficult due to scatterer MTRC and slow-time-dependent Doppler frequecies f_p.

To choose a suitable CPI for the image reconstruction, a so-called time window optimization procedure can be used. Its purpose is to locate a slow-time window during which the target rotational motion is as uniform as possible. In its most simple form, it chooses a single time window (length and location) from the entire recorded slow-time signal, which is then used in the RD imaging method. More generally, the optimization can be seen as a method for optimizing the parameters of the TFR that is used in the RID image reconstruction [15], [130].

Martorella *et al.* proposed choosing the slow-time window by maximizing the image contrast when using the RD method [197]. Another possibility is to estimate the instantaneous Doppler of different scatterers on the target, as demonstrated in [198]. These procedures are useful in cases where the target exhibits complex motions and the direction of the rotation changes, such as in imaging maritime targets [199]–[205]. More recently, the time window optimization procedure has been used to image ground and air targets as well [15], [130], [206].

The time window optimization is technically not a motion compensation procedure, since it does not produce estimates for the target motion. However, it has been shown to be a useful technique to avoid more complicated estimation strategies and thus to produce a computationally feasible approach for reconstructing images with sufficient cross-range resolution and focusing quality.

TABLE 4. Advantages and disadvantages of different cross-range scaling methods.

Method	Advantages	Disadvantages
Optimization-based	Do not require isolated dominant scatterers Information of the entire image is used	High computational cost Usually limited to uniform rotation
Phase estimation-based	Computationally efficient Not limited to uniform rotation	Require multiple isolated dominant scatterers More sensitive to low SNR

Cross-Range Scaling

When using the above-mentioned RD, RID, or any other Doppler frequency estimation-based approaches for the image reconstruction, the target rotational motion parameters (θ as a function of slow-time) are usually not explicitly estimated. For properly interpreting the ISAR image, it is necessary to know the image projection plane and the spatial scale of the cross-range axis. The rotational motion parameters determine the relationship between the Doppler frequency and the cross-range position of the scatterers. The procedure of estimating the target rotation during the CPI – referred to as cross-range scaling – is a very difficult task with no general solution.

Several cross-range scaling methods based on estimating the slow-time phase history of multiple dominant point scatterers have been proposed in [17], [207]–[218]. These methods utilize the relationship between the higher order phase coefficients the cross-range location and the rotational velocity of the scatterers. The second or third order phase coefficients are obtained by isolating point scatterers and estimating their phase as a function of slow-time. Because the phase estimation approaches are not usually directly applicable to RID image reconstruction, a suitable approach for incorporating them has recently been considered in [219].

Another class of algorithms is based on optimizing a suitable objective function to estimate the target rotation. The optimization-based methods divide the CPI into two or more parts to produce sub-aperture images of the target. These images can be considered as scaled and rotated versions of each other. Thus, maximizing their correlation can be used to estimate the rotation between them. This provides an estimate for the target rotation between the sub-aperture images. For example, the rotation correlation and polar mapping methods [220], [221] are based on maximizing the correlation between two sub-aperture images as a function of the rotation applied to one of them.

More recently, approaches that try to extract features (e. g. dominant point scatterers or lines) from sub-aperture images and correlate them instead of the entire images have been proposed [222]–[228]. The sub-aperture technique has also been used to obtain 3-D locations for the target scatterers [229], and a cross-range scaling approaches have recently been proposed for this application [230], [231]. Another possible way is to maximize the image contrast based on the rotational motion model used in the slow-time matched filtering [232]–[234].

Of the above-mentioned two classes, the phase estimation-based approaches require usually at least three range bins that contain a single isolated dominant scatterer with high SNR. When this assumption is not fulfilled, the phase estimation accuracy (and consequently also the cross-range scaling accuracy) significantly degrades. The optimization-based approaches are more generally applicable, since they do not require the isolation of dominant scatterers. On the contrary, they work best when the target reflectivity distribution is more even, highly dominant scatterers may even degrade their performance. As a drawback, the required optimization algorithms are often computationally intensive and do not guarantee that the global optimum is found. Moreover, the use of sub-aperture images (or features) works ideally only when the rotation is uniform, since non-uniform rotation causes a different scaling factor and defocusing between the sub-aperture images.

Thus, the choice of a suitable cross-range scaling method depends on the expected target type and motion dynamics. The strengths and weaknesses of the above-descrobed two algorithm classes are summarized in Table 4.

C. DISCUSSION

Even though the single-step approach in translational motion compensation is generally more robust than range alignment followed by autofocus, its use has been limited mainly due to the higher computational cost. However, as the desired image resolution gets higher, it becomes necessary to abandon the more efficient two-step approach. Moreover, the single-step approach is often more straightforward to implement, because each of the range alignment and autofocusing algorithms have their own tunable parameters and limitations.

The two-step approach (image reconstruction filter and cross-range scaling) in rotational motion compensation is fairly robust against different scenarios. It should be noted, that the RID imaging approach offers some robustness even against residual translational motion errors. Cross-range scaling is performed independently and usually does not rely on the previous motion compensation steps to work properly. BP performs the image reconstruction and cross-range scaling in one step (since the rotation is explicitly used in the image reconstruction filter). However, currently there are no generally applicable computationally feasible approaches incorporating data-driven motion compensation in BP.

Reference [15] demonstrated the full ISAR processing chain consisting of range alignment, autofocus, RID imaging and cross-range scaling using the state-of-the-art algorithms in each of the aforementioned steps. The results indicated that an image resolution of about 10–15 cm was possible to achieve in X-band even in complicated target motion scenar-

ios including highly non-linear translation and rotation. To increase the resolution beyond 10 cm, the approximations of the step-wise approach start to break down and a more general method such as BP is required.

V. SPATIALLY DISTRIBUTED ISAR

Spatially distributed systems can be used to solve certain problems that are inherent in monostatic ISAR. For example, a distributed configuration is robust against unfortunate imaging geometries: A target that approaches a monostatic radar radially cannot be imaged in cross-range, because all the scatterers have the same Doppler frequency f_p. Moreover, obtaining images from multiple aspect angles gives important additional information about the target reflectivity. A 3-D imaging capability is also obtained by using receivers at different heights. This information is of crucial importance in NCTR applications. On the other hand, multistatic systems are more complex and require additional considerations suh as precise synchronization between the radar stations. These challenges, as well as additional comparisons between monostatic and multistatic ISAR have been analyzed in [235].

This sections reviews the most important spatially distributed ISAR system concepts and the associated processing algorithms. Section V-A surveys the early references of bi- and multistatic systems. An interesting and important special case of bistatic systems is passive bistatic ISAR, which is reviewed in Section V-B. Section V-C investigates spatially distributed systems capable of locating target scatterers in 3-D using interferometric techniques.

A. BI- AND MULTISTATIC ISAR

Early theoretical developments, including a bistatic ISAR signal model and analysis concerning the resolution and geometrical distortions were presented in references [236]–[238]. As an important result, it was shown that under certain conditions the bistatic configuration can be approximated as an equivalent monostatic setup, which greatly simplifies the ISAR processing [237]. However, as a drawback, this approximation causes geometric distortions and thus makes the interpretation of the bistatic ISAR images more difficult.

More recent developments of bistatic ISAR include dedicated motion compensation methods [239], a system with a ship-borne receiver and a shore-based transmitter with associated imaging and motion estimation algorithms [240], and techniques to mitigate the distortions caused by the monostatic approximation [241]–[244].

Early experimental results obtained with multistatic ISAR were reported in [245]. Theoretical developments of multistatic ISAR image reconstruction and resolution analysis along with experimental demonstrations followed in [246]. Further theoretical considerations related to multistatic motion compesation and image reconstruction were later published in [247], [248]. Brisken *et al.* developed an experimental multistatic ISAR imaging system (FEMMES) and demonstrated the motion estimation and imaging techniques in a series of publications [18], [249]–[253]. The FEMMES system is capable of forming multistatic images in X-band with approximately 10 cm resolution. This research demonstrated the entire multistatic processing chain, starting from the synchronization using the direct path signal all the way up to the multilateration-based motion estimation and BP-based image reconstruction.

The multistatic ISAR concept makes the motion compensation problem more tractable, since the additional receivers provide new information for the data-driven estimation algorithms. However, multistatic systems are currently not very common due to the required system complexity. With developing radar technology and the increased interest in fully coherent multiple-input-multiple output (MIMO) techniques, multistatic ISAR has potential to become ubiquitous in new ISAR applications.

B. PASSIVE BISTATIC ISAR

In recent years, passive radars have received a great deal of interest in the scientific community. Passive systems have several advantages over active systems, such as reduced cost, low vulnerability to electronic countermeasures, low probability of intercept, wide coverage areas, and continuous signal acquisition. These systems use different types of electromagnetic sources called illuminators of opportunity. They can be for example active radar, communications, navigation or digital broadcasting transmitters. As a drawback, the waveform is not under the operator's control, and thus the achievable range resolution may be inadequate for high-resolution imaging.

Problems specific to passive ISAR are the often relatively poor range resolution (due to the limited bandwidth of conventional illuminators of opportunity) and the estimation of complex target motions. Due to the poor range resolution, small targets typically cannot be resolved in range – their response falls into a single range bin. Thus, the ISAR images obtained by passive ISAR systems are usually in the form of 1-D cross-range profiles. The low carrier frequency of typical illuminators requires a very long CPI to be processed for obtaining good cross-range resolution. This poses strict requirements for the motion estimation and compensation, which is a prerequisite for successful cross-range imaging.

The first demonstrations of passive radar imaging were in the context of airborne SAR. References [254]–[256] presented methods for obtaining images of moving targets in passive SAR images. In the early 2010s, the first passive ISAR applications using Global System for Mobile (GSM) and digital broadcasting signals for imaging air- and maritime targets were published in [257]–[261]. As an early theoretical development, [262] proposed a passive ISAR imaging method for point targets relying on a test of a binary hypothesis, which was used to determine the target position and velocity.

Martorella *et al.* [263] presented the first rigorous theoretical development of passive bistatic ISAR imaging. A more recent pair of papers by Garry *et al.* describes several additional theoretical and practical considerations, such as motion

TABLE 5. Advantages and disadvantages of spatially distributed ISAR systems.

Advantages	Disadvantages
Robustness to unfortunate imaging geometries (target motions)	Increased hardware complexity and cost
Increased image information content through diverse observation perspectives	Need for precise time and phase synchronization
Additional degrees of freedom for data-driven motion estimation	Increased algorithm and computational complexity
	Increased data rate and volume

compensation and using different illuminators of opportunity [264], [265]. Colone *et al.* [266], [267] published the first comprehensive demonstration of the passive ISAR processing chain with WiFi- and very high frequency (VHF)-based experimental data. The processing chain for passive radar is in many ways more complicated than for active monostatic radars. This is because range compression and clutter cancellation require a more sophisticated approach. More recently, a number of passive ISAR experiments using digital television (DTV), digital video broadcasting (DVB-T and DVB-S) signals have been reported in [190], [268]–[273]. Additionally, global navigation satellite systems (GNSS) signals have also been used for passive ISAR in [274]–[276].

C. 3-D INISAR

Spatially distributed ISAR systems can be used as interferometric systems to estimate the 3-D positions of the target scatterers. In these systems, the setup is either bi-, multi-, or quasi-monostatic. The important aspect needed for the 3-D localization capability is have at least two receive (RX) antennas, which are separated in the elevation direction. This way, the phase differences between the RX channels can be used to estimate the height of the scatterers – using the same principle that has been widely used in cross-track interferometic SAR systems, e. g. to produce digital elevation models of the ground surface. An important limitation of interferometry is that only a single scatterer can occupy the same range-cross-range resolution cell.

The earliest applications of the 3-D InISAR reconstruction were proposed in the late 1990s and early 2000s in [277]–[281]. Since, then it has matured into a well-established technique, with numerous papers describing its theory and reconstruction algorithms [282]–[291]. Several applications, including maritime target imaging [292]–[294], aircraft imaging [295], and FMCW ISAR [296] have been reported. Most recently, the 3-D InISAR concept has also been demonstrated using passive bistatic ISAR [297].

The aforementioned references mostly deal with the quasi-monostatic setup, where closely spaced RX antennas are used to obtain 3-D estimates of scatterer positions. The images from the individual RX channels are combined to achieve better estimates of the target's dimensions. As previously mentioned, the quasi-monostatic setup has certain drawbacks (e. g., related to unfortunate imaging geometries). For this reason, 3-D InISAR has more recently been considered for spatially distributed bi- and multistatic setups [298]–[300]. These techniques are based on fusing the information contained in the 2-D images obtained from different RX stations of the multistatic setup to estimate the 3-D scatterer locations.

Besides the 3-D capability, these InISAR systems have an additional attractive ability: They can be used to estimate the direction of the target rotation vector. Monostatic systems can only resolve the magnitude of the rotation, not the direction. Because the direction of the rotation vector determines the image projection plane in 2-D imaging, its estimation is highly important for image interpretation and NCTR. References [301]–[306] describe techniques for estimating the rotation vector from multisensor measurements.

Table 5 summarizes the various aspects of using spatially distributed ISAR systems. The listed advantages make these techniques an important trend in ISAR with increasing research interest. The disadvantages related to system complexity are becoming less of an issue due to the developing technology.

VI. RECENT ISAR APPLICATIONS

Since the early days of ISAR, the most important applications have been in the military context, e. g., imaging ships, ground vehicles, and aircraft. Nowadays, the developing radar technology makes ISAR a more attractive concept in other applications as well. This section surveys a number of recent important application areas of ISAR: ground moving target imaging from an airborne platform, imaging targets with internal motion, and space surveillance.

The timeline of Figure 5 summarizes the most significant ISAR applications and algorithmic developments since the 1990s including the methods described in Sections V– VII.

A. GROUND MOVING TARGET IMAGING

ISAR can be used to image targets moving on Earth's surface using a space- or airborne SAR sensor. This concept was first demonstrated in Raney's paper [46], and it has attracted a great deal of interest more recently [13]. For this application, there is an additional challenge besides motion compensation: The strong ground clutter returns may mask the moving target reflections. For this purpose, multichannel systems that are able to cancel the ground clutter returns and detect the moving targets are commonly used.

An early method for performing motion compensation in this application was the prominent point processing method [2], [49], where the slow-time phase of multiple dominant scatterers was estimated to compensate the target motion. Another method proposed by Fienup [307] used a sharpness maximization procedure to focus patches of the SAR image that contained smeared moving target returns. Keystone formatting was initially proposed to compensate the

moving target translation in SAR images [62]. Combined with an autofocus algorithm, this approach was demonstrated to produce focused moving target images in [308], [309]. Another more general motion compensation approach was proposed and demonstrated in [310]. All of these methods were designed for single-channel systems. Moreover, they assume the moving target reflections to be much stronger than the ground clutter returns.

More recently, the problem has been approached by using the conventional ISAR processing scheme after isolating and projecting the moving target signal from the SAR image into the range-slow-time domain. Experimental demonstrations with Cosmo-SkyMed data using this approach have been reported in [311]–[313]. Furthermore, a frequency domain focusing algorithm and experimental demonstration with airborne data were reported in [314], [315].

When imaging weakly reflecting targets, the cancellation of the ground clutter signal is a prerequisite for successful ISAR image reconstruction. A common method for this purpose is space-time adaptive processing (STAP) [316], which can be used for systems with multiple RX channels. An approach combining STAP and ISAR processing has been developed and demonstrated in references [317]–[322]. Additionally, a virtual multichannel approach, i, e., using a single-channel system to emulate a multichannel system, has been used and compared to actual multichannel systems in [323].

Ground moving target detection with airborne radar using STAP is a well-established technique. Adding the capability of ISAR imaging to this technology offers the possibility to obtain a significantly improved situational awareness. The targets can not only be detected and located, but possibly also classified or recognized based on their ISAR signatures. This application presents a novel algorithmic challenge, because the SNR (or more precisely the signal-to-clutter ratio, SCR) is often much lower than in conventional ISAR processing. Even though the STAP-ISAR approach shows promise, much work remains to be done to make this concept more robust and generally applicable.

B. IMAGING TARGETS WITH ROTATING PARTS

In conventional ISAR processing, the target is assumed to be a rigid body. Under this assumption, the position of each target scatterer depends only on the rotation $\theta(t)$ of the rigid target. However, certain common ISAR targets, such as helicopters, aircraft, and drones contain rapidly rotating parts, violating the rigid body assumption. For example, the extremely fast rotation of rotor blades causes highly non-stationary Doppler frequency modulation, which makes it very difficult to obtain a focused ISAR image of the target. Even if the translation and the rotation of the rigid part of the target are properly estimated and compensated, the micro-Doppler caused by the non-rigid rotating part may blur and defocus the entire image. Moreover, the blurred rotating part echo may mask important rigid body target features.

To overcome the aforementioned problem, several methods for separating the rigid body and rotating part reflections have been considered in the ISAR literature. On the time-frequency plane, the rigid body echoes follow straight lines whereas the rotating parts follow a sinusoidal curve. Fundamentally, all of the separation methods are in some way based on using this qualitative difference in the time-frequency behavior of the echoes.

An early development based on using a TFR and order statistics to obtain the rotating part signals was proposed in [324]. This approach was further developed, analyzed, and demonstrated in later publications [325]–[327]. An approach based on this concept but using a procedure to improve the time-frequency resolution has been proposed in [328].

Other separation methods have since been proposed, e. g., based on the Hough transform [329], [330] and the Radon transform [331]. Various approaches based on using different decomposition methods from linear algebra have also been used for this purpose: principal component analysis [332], empirical mode decomposition [333], complex local mean decomposition [334], and bivariate variational mode decomposition [335].

The methods for imaging non-rigid targets with rotating parts are an important extension to ISAR imaging. Besides enabling successful imaging of new targets in old applications, these techniques may open up new potential application areas, such as imaging moving persons.

C. SPACE SURVEILLANCE

As the number of operating and defunct satellites orbiting the Earth is continuously increasing, the risk of collisions between active satellites and space debris becomes more pronounced. Thus, it is increasingly important to have an accurate situational awareness of near-Earth space. A number of radar systems have recently been developed to improve space surveillance capabilities. Some of these systems are low resolution and only provide a capability to detect and track targets. Others are capable of high-resolution ISAR imaging, providing an important information source for monitoring and characterizing the observed satellites.

The earliest space surveillance systems LRIR and ALCOR were developed in the 1970s, as previously described in Section III. Since then, the Lincoln Laboratory has developed the Ku-band Haystack Auxiliary (HAX) system with 13 cm range resolution and the Ka-band Millimeter-Wave (MMW) radar with 7 cm resolution [336]. Most recently, the W-band Haystack Ultrawideband Satellite Imaging Radar (HUSIR) has been put to operational use [336]. It can produce ISAR images with an extremely high resolution of approximately 2 cm, representing the absolute state-of-the-art in long-range non-cooperative ISAR imaging performance.

Another high performance space surveillance radar system is the Tracking and Imaging Radar (TIRA) developed by Fraunhofer FHR [337], [338]. This Ku-band system is capable of producing decimeter resolution ISAR images of satellites. The reconstructed images have recently been used

to analyze the rotation of ENVISAT [7] and to monitor the uncontrolled re-entry of the Tiangong-1 satellite [339]. The most recent new space surveillance radar with high-resolution ISAR imaging capability is the X-band Imaging of Satellites in Space (IoSiS) system [8] developed by the German Aerospace Center. While still in its commissioning phase, the system has already produced high-resolution ISAR images of the International Space Station (ISS) [8], [340].

As space surveillance is becoming an increasingly important task, ISAR techniques will be pushed forward by the requirements to detect and identify very small objects (various space debris particles) with extremely high resolution. The fast motion and uncontrolled rotation of space debris particles poses a novel challenge for ISAR motion compensation algorithms.

VII. RECENT ALGORITHMIC DEVELOPMENTS

During recent years, there has been great research interest in CS and ML techniques. In addition to theoretical developments in these fields, they have been used in an increasing number of engineering applications. In this section, we survey their use in ISAR imaging.

A. CS IN ISAR

The ISAR imaging problem can be formulated as a linear inverse problem where the unknown target reflectivity distribution (RCS as a function of spatial position) is reconstructed from noisy measurements of scattered electromagnetic signals. CS techniques exploit the sparsity of the target signal to find sparse solutions to the under-determined linear equations that constitute the imaging problem. The simplest form of sparsity is to consider the target as a small number of dominant point scatterers – often an accurate assumption in ISAR.

The CS algorithms can reconstruct the target image with suppressed sidelobes and increased spatial resolution of point scatterers (super-resolution). Furthermore, CS provides increased robustness to limitations in the data quality and quantity. Typical data limitations include missing pulses, sparse frequency spectrum waveforms, etc. Thus, CS can significantly increase the ISAR image quality, providing enhanced target information for a subsequent NCTR or ATR stage.

The use of CS techniques in SAR and other radar imaging applications has been reviewed in references [341], [342]. These papers provide a concise theoretical description of the image reconstruction procedure. Moreover, they discuss various practical considerations and CS-based radar imaging applications. However, both of these papers are mainly focused on SAR – only a few ISAR references are given. To fill in this gap, we proceed to survey the CS-based methods used in the context of ISAR imaging.

The CS-based approach is useful in situations where the available radar data is incomplete or non-uniformly sampled – e. g., pulses are missing, the target rotates rapidly and non-uniformly, frequencies are missing due to jamming, etc. References [343]–[351] demonstrate ISAR image reconstruction using CS when a number of pulses (range profiles) is missing, i.e., in case of sparse slow-time sampling. References [352]–[354] propose CS-based methods to deal with the sparse angular sampling caused by a rapid target rotation. Another possibility is to use sparse sampling in the waveform by using a sparse stepped frequency waveform [355]–[357]. This approach can be beneficial in applications where covert radar operation with a low probability of intercept is required.

The CS-based image reconstruction has been found to be useful in 3-D InISAR processing [358]. Moreover, it is useful in the case of multistatic 3-D ISAR imaging, because it offers a way to avoid the coherent combination of the signals from the different RX stations [253], [359]. Examples of CS-based 3-D InISAR imaging methods can be found in references [360], [361]. Furthermore, specific methods and results have been presented for space [354], [362], maritime [358] and general maneuvering target [363], [364] imaging.

An important feature of CS is its capability to enhance the image resolution. Approaches where the achievable image resolution no longer only depends on the signal bandwidth and target rotation are commonly referred to as super-resolution techniques. Reference [365] presents comparisons between CS and other super-resolution techniques in ISAR. A number of different CS methods have been used for this purpose: sparse Bayesian learning [366]–[373], the RELAX method [374], matching pursuit [375], and dictionary learning [376], [377].

In ISAR processing, the unknown target motion usually hinders the direct application of CS-based reconstruction techniques. Moreover, the motion compensation approaches described in the previous sections are usually not directly applicable: They have been designed for linear reconstruction methods and Nyquist sampled data. Thus, several approaches for performing data-driven motion compensation for CS-based ISAR have been developed. For example, the image sharpness maximization can be included in the CS optimization problem [378]. It is also possible to include the unknown phase errors in addition to the sparse scattering coefficients in the CS optimization problem formulation. This approach demonstrated in references [379]–[385] is equivalent to joint image reconstruction and autofocusing.

Despite the potential and voluminous literature on the subject, CS-based ISAR imaging in operational systems is still very limited. Most of the reported results deal with idealized simulation scenarios or simple, closely controlled target scenarios. The reviewed methods require stringent approximations to hold in order to produce meaningful ISAR images. Thus, their performance heavily depends on a favorable target scenario. Moreover, CS-based approaches generally require a high SNR to provide useful results and the computational complexity is often much higher than for the linear image reconstruction and motion compensation methods described in the previous sections. Table 6 presents a summary of the aforementioned advantages and disadvantages of the CS-based ISAR imaging approaches.

TABLE 6. Advantages and disadvantages of CS-based ISAR methods.

Advantages	Disadvantages
Super-resolution capability	Increased processing complexity
Easier 3-D multistatic image formation and fusion	Need for a priori assumptions about target reflectivity (sparse point scatterer model)
Increased robustness in case of sparsely sampled or missing data	Requires a high SNR
Suppressed image sidelobes	Difficult to integrate with computationally efficient motion compensation

B. ML IN ISAR

The recent developments in computing power and ML techniques are making their way into ISAR. Previously, the use of ML in the context of ISAR has been limited to NCTR and ATR, i. e., classifying targets based on the reconstructed images. This subject is out of the scope of this review (for a relatively recent review of ATR techniques, see [386]).

During the last few years, a number of methods using ML techniques in ISAR image reconstruction have been proposed. In [387]–[389], the authors used a convolutional neural network (CNN) to reconstruct ISAR images from sparsely sampled data and demonstrated the improved performance compared to CS-based ISAR. Furthermore, an autofocus approach has been integrated into the CNN framework in [390]. Neural networks have also recently been used to enhance the image resolution [391], [392]. Additionally, the CNN-based approach has recently been demonstrated in the ground moving target imaging application [393].

The inherent challenge in ML-based imaging approaches is the need for a large amount of representative training data. In the radar application, it is notoriously difficult to obtain comprehensive training data: The RCS modeling and simulation for different aspect angles and frequencies is cumbersome and requires accurate target models, which are not readily available for all possible targets. Moreover, sharing and obtaining data is quite restricted for military targets.

As an advantage, a proper ML architecture avoids all the conventional challenges with ISAR processing: By incorporating the unknown motion dynamics in the training data, the neural network performs all the required processing without a need to explicitly design separate motion estimation algorithms. In conclusion, despite the promising concept, ML-based ISAR imaging is still in its infancy.

VIII. CONCLUSION

This paper has presented a comprehensive literature survey of ISAR imaging techniques and applications from the late 1950s to present day. The timelines of Figures 4 and 5 summarize the important technical milestones described in this paper. After introducing the basic ISAR principles and terminology, we described the early historical developments starting from the imaging of the Moon and planets, continuing to early algorithmic developments and imaging airborne targets. Then, we proceeded to analyze the various methods used for motion compensation and image reconstruction in monostatic ISAR processing. We continued by analyzing spatially distributed ISAR concepts, which offer various advantages and hold great potential for future ISAR developments. We proceeded by describing important current applications including ground moving target imaging, non-rigid target imaging, and space surveillance. Finally, we surveyed the ISAR literature using the latest developments from CS and ML.

In general, non-cooperative ISAR imaging is a very challenging task with no general purpose solution – hence the voluminous literature on the subject. However, the increasing computational resources allow the development of more generally applicable algorithms and the use of CS and ML techniques. To provide images with increased information content, the trend of ISAR is moving towards spatially diverse systems and higher spatial resolution. The rapid development of affordable high-resolution radar systems continually opens up new possible application areas for ISAR imaging, transforming from a niche field to the mainstream.

REFERENCES

[1] J. C. Curlander and R. N. McDonough, *Synthetic aperture radar*. Wiley, New York, 1991, vol. 11.
[2] W. G. Carrara, R. S. Goodman, and R. M. Majewski, *Spotlight Synthetic Aperture Radar: Signal Processing Algorithms*. Boston, MA: Artech House, 1995.
[3] C. V. Jakowatz Jr., D. Wahl, P. Eichel, D. Ghiglia, and P. Thompson, *Spotlight-mode Synthetic Aperture Radar: A signal processing approach*. Boston, MA: Kluwer Academic Publishers, 1996.
[4] S. M. Patole, M. Torlak, D. Wang, and M. Ali, "Automotive radars: A review of signal processing techniques," *IEEE Signal Processing Magazine*, vol. 34, no. 2, pp. 22–35, Mar. 2017.
[5] S. Brisken, F. Ruf, and F. Höhne, "Recent evolution of automotive imaging radar and its information content," *IET Radar, Sonar & Navigation*, vol. 12, no. 10, pp. 1078–1081, Oct. 2018.
[6] J. Ender, L. Leushacke, A. Brenner, and H. Wilden, "Radar techniques for space situational awareness," in *2011 12th International Radar Symposium (IRS)*. IEEE, 2011, pp. 21–26.
[7] S. Sommer, J. Rosebrock, D. Cerutti-Maori, and L. Leushacke, "Temporal analysis of ENVISAT's rotational motion," in *7th European Conference on Space Debris, ESA/ESOC, Darmstadt/Germany*, 2017.
[8] S. Anger, M. Jirousek, S. Dill, and M. Peichl, "IoSiS – a high performance experimental imaging radar for space surveillance," in *2019 IEEE Radar Conference (RadarConf)*, Apr. 2019, pp. 1–4.
[9] V. C. Chen and H. Ling, *Time-frequency transforms for radar imaging and signal analysis*. Artech House, 2002.
[10] V. C. Chen and M. Martorella, *Inverse Synthetic Aperture Radar Imaging: Principles, Algorithms and Applications*. Institution of Engineering and Technology, 2014.
[11] M. Martorella, "Introduction to inverse synthetic aperture radar," in *Academic Press Library in Signal Processing*. Elsevier, 2014, vol. 2, pp. 987–1042.
[12] C. Ozdemir, *Inverse synthetic aperture radar imaging with MATLAB algorithms*. John Wiley & Sons, 2021.
[13] M. Martorella, S. Gelli, and A. Bacci, "Ground moving target imaging via SDAP-ISAR processing: Review and new trends," *Sensors*, vol. 21, no. 7, p. 2391, 2021.
[14] "IEEE standard for radar definitions," *IEEE Std 686-2017 (Revision of IEEE Std 686-2008)*, pp. 1–54, Sep. 2017.
[15] R. Vehmas, J. Jylhä, M. Väilä, J. Vihonen, and A. Visa, "Data-driven motion compensation techniques for noncooperative ISAR imaging,"

IEEE Transactions on Aerospace and Electronic Systems, vol. 54, no. 1, pp. 295–314, Feb. 2018.

[16] D. C. Munson, J. D. O'Brien, and W. K. Jenkins, "A tomographic formulation of spotlight-mode synthetic aperture radar," *Proceedings of the IEEE*, vol. 72, no. 8, pp. 917–925, Aug. 1983.

[17] M. Martorella, "Novel approach for ISAR image cross-range scaling," *IEEE Transactions on Aerospace and Electronic Systems*, vol. 44, no. 1, pp. 281–294, Jan. 2008.

[18] S. Brisken, M. Martorella, T. Mathy, C. Wasserzier, J. G. Worms, and J. H. G. Ender, "Motion estimation and imaging with a multistatic ISAR system," *IEEE Transactions on Aerospace and Electronic Systems*, vol. 50, no. 3, pp. 1701–1714, Jul. 2014.

[19] D. A. Ausherman, A. Kozma, J. L. Walker, H. M. Jones, and E. C. Poggio, "Developments in radar imaging," *IEEE Transactions on Aerospace and Electronic Systems*, vol. AES-20, no. 4, pp. 363–400, Jul. 1984.

[20] R. Price and P. E. Green Jr, "Signal processing in radar astronomy," *MIT Lincoln Lab. Report No. 234*, 1960.

[21] I. I. Shapiro, "Planetary radar astronomy," *IEEE Spectrum*, vol. 5, no. 3, pp. 70–79, 1968.

[22] L. J. Porcello, C. E. Heerema, and N. G. Massey, "Optical processing of planetary radar data: preliminary results," *Journal of Geophysical Research*, vol. 74, no. 4, pp. 1111–1115, 1969.

[23] T. Hagfors and D. B. Campbell, "Mapping of planetary surfaces by radar," *Proceedings of the IEEE*, vol. 61, no. 9, pp. 1219–1225, 1973.

[24] G. H. Pettengill, "Measurements of lunar reflectivity using the Millstone radar," *Proceedings of the Institute of Radio Engineers*, vol. 48, no. 5, pp. 933–934, 1960.

[25] J. H. Thomson, J. E. B. Ponsonby, G. N. Taylor, and R. S. Roger, "A new determination of the solar parallax by means of radar echoes from Venus," *Nature*, vol. 190, no. 4775, pp. 519–520, 1961.

[26] L. R. Malling and S. Golomb, "Radar measurements of the planet Venus," *Journal of the British Institution of Radio Engineers*, vol. 22, no. 4, pp. 297–300, 1961.

[27] W. B. Smith, "Radar observations of Venus, 1961 and 1959," *The Astronomical Journal*, vol. 68, p. 15, 1963.

[28] R. L. Carpenter and R. M. Goldstein, "Radar observations of Mercury," *Science*, vol. 142, no. 3590, pp. 381–382, 1963.

[29] J. V. Evans, R. A. Brockelman, J. C. Henry, G. M. Hyde, L. G. Kraft, W. A. Reid, and W. W. Smith, "Radio echo observations of Venus and Mercury at 23 cm wavelength," *The Astronomical Journal*, vol. 70, p. 486, 1965.

[30] R. M. Goldstein, "Radar observations of Mercury," *The Astronomical Journal*, vol. 76, p. 1152, 1971.

[31] R. B. Dyce, "Recent Arecibo observations of Mars and Jupiter," *Journal of Research of the National Bureau of Standards D*, vol. 69, p. 1628, 1965.

[32] L. A. Hoffman, K. H. Hurlbut, D. E. Kind, and H. J. Wintroub, "A 94-GHz radar for space object identification," *IEEE Transactions on Microwave Theory and Techniques*, vol. 17, no. 12, pp. 1145–1149, 1969.

[33] R. K. Avent, J. D. Shelton, and P. Brown, "The ALCOR C-band imaging radar," *IEEE Antennas and Propagation Magazine*, vol. 38, no. 3, pp. 16–27, Jun. 1996.

[34] D. R. Bromaghim and J. P. Perry, "A wideband linear FM ramp generator for the long-range imaging radar," *IEEE Transactions on Microwave Theory and Techniques*, vol. 26, no. 5, pp. 322–325, May 1978.

[35] W. M. Brown, "Synthetic aperture radar," *IEEE Transactions on Aerospace and Electronic Systems*, vol. AES-3, no. 2, pp. 217–229, Mar. 1967.

[36] W. M. Brown and R. J. Fredricks, "Range-Doppler imaging with motion through resolution cells," *IEEE Transactions on Aerospace and Electronic Systems*, vol. AES-5, no. 1, pp. 98–102, Jan. 1969.

[37] J. L. Walker, W. G. Carrara, and I. Cindrich, "Optical processing of rotating-object radar data using a polar recording format," Rome Air Development Center, Rome, NY, Tech. Rep. RADC-TR-73-136, AD 526 738, May 1973.

[38] J. L. Walker, "Range-Doppler imaging of rotating objects," *IEEE Transactions on Aerospace and Electronic Systems*, vol. AES-16, no. 1, pp. 23–52, Jan. 1980.

[39] R. Voles, "Radar target imaging by rotation about two axes," in *Proceedings of the Institution of Electrical Engineers*, vol. 125, no. 10. IET, 1978, pp. 919–921.

[40] M. Prickett and C. Chen, "Principles of inverse synthetic aperture radar/ISAR/imaging," in *EASCON'80; Electronics and Aerospace Systems Conference*, 1980, pp. 340–345.

[41] D. Mensa, G. Heidbreder, and G. Wade, "Aperture synthesis by object rotation in coherent imaging," *IEEE Transactions on Nuclear Science*, vol. 27, no. 2, pp. 989–998, Apr. 1980.

[42] D. L. Mensa, S. Halevy, and G. Wade, "Coherent Doppler tomography for microwave imaging," *Proceedings of the IEEE*, vol. 71, no. 2, pp. 254–261, Feb. 1983.

[43] D. R. Wehner, M. J. Prickett, R. G. Rock, and C. C. Chen, "Stepped frequency radar target imagery, theoretical concept and preliminary results," Naval Ocean Systems Center, San Diego, CA, Tech. Rep. 490, Nov. 1979.

[44] C. C. Chen and H. C. Andrews, "Target-motion induced radar imaging," *IEEE Transactions on Aerospace and Electronic Systems*, vol. AES-16, no. 1, pp. 2–14, Jan. 1980.

[45] ——, "Multifrequency imaging of radar turntable data," *IEEE Transactions on Aerospace and Electronic Systems*, vol. AES-16, no. 1, pp. 15–22, Jan. 1980.

[46] R. K. Raney, "Synthetic aperture imaging radar and moving targets," *IEEE Transactions on Aerospace and Electronic Systems*, vol. AES-7, no. 3, pp. 499–505, May 1971.

[47] K. Wu and M. Vant, "A SAR focusing technique for imaging targets with random motion," *NAECON 1984*, pp. 289–295, 1984.

[48] A. Freeman and A. Currie, "Synthetic aperture radar (SAR) images of moving targets," *GEC Journal Research*, vol. 5, no. 2, pp. 106–115, 1987.

[49] S. Werness, W. Carrara, L. Joyce, and D. Franczak, "Moving target imaging algorithm for SAR data," *IEEE Transactions on Aerospace and Electronic Systems*, vol. 26, no. 1, pp. 57–67, Jan. 1990.

[50] S. Barbarossa, "Detection and imaging of moving objects with synthetic aperture radar. Part 1: Optimal detection and parameter estimation theory," *IEE Proceedings F (Radar and Signal Processing)*, vol. 139, no. 1, pp. 79–88, Feb. 1992.

[51] S. Barbarossa and A. Farina, "Detection and imaging of moving objects with synthetic aperture radar. Part 2: Joint time-frequency analysis by Wigner-Ville distribution," *IEE Proceedings F (Radar and Signal Processing)*, vol. 139, no. 1, pp. 89–97, Feb. 1992.

[52] K. D. Ward, R. J. A. Tough, and B. Haywood, "Hybrid SAR-ISAR imaging of ships," in *IEEE International Conference on Radar*. IEEE, 1990, pp. 64–69.

[53] B. D. Steinberg, "Microwave imaging of aircraft," *Proceedings of the IEEE*, vol. 76, no. 12, pp. 1578–1592, Dec. 1988.

[54] B. Steinberg, "Radar imaging from a distorted array: The radio camera algorithm and experiments," *IEEE Transactions on Antennas and Propagation*, vol. 29, no. 5, pp. 740–748, Sep. 1981.

[55] B. Haywood and R. J. Evans, "Motion compensation for ISAR imaging," in *ASSPA 89*, Apr. 1989, pp. 113–117.

[56] G. Y. Delisle and H. Wu, "Moving target imaging and trajectory computation using ISAR," *IEEE Transactions on Aerospace and Electronic Systems*, vol. 30, no. 3, pp. 887–899, Jul. 1994.

[57] H. Wu, D. Grenier, G. Y. Delisle, and D.-G. Fang, "Translational motion compensation in ISAR image processing," *IEEE Transactions on Image Processing*, vol. 4, no. 11, pp. 1561–1571, Nov. 1995.

[58] H. Wu and G. Y. Delisle, "Precision tracking algorithms for ISAR imaging," *IEEE Transactions on Aerospace and Electronic Systems*, vol. 32, no. 1, pp. 243–254, Jan. 1996.

[59] J. M. Munoz-Ferreras and F. Perez-Martinez, "Extended envelope correlation for range bin alignment in ISAR," in *2007 IET International Conference on Radar Systems*, Oct. 2007, pp. 1–5.

[60] Y. Lu, J. Yang, Y. Zhang, and S. Xu, "Noise-robust range alignment method for inverse synthetic aperture radar based on aperture segmentation and average range profile correlation," *EURASIP Journal on Advances in Signal Processing*, vol. 2021, no. 1, pp. 1–20, 2021.

[61] T. Sauer and A. Schroth, "Robust range alignment algorithm via Hough transform in an ISAR imaging system," *IEEE Transactions on Aerospace and Electronic Systems*, vol. 31, no. 3, pp. 1173–1177, Jul. 1995.

[62] R. P. Perry, R. C. DiPietro, and R. L. Fante, "SAR imaging of moving targets," *IEEE Transactions on Aerospace and Electronic Systems*, vol. 35, no. 1, pp. 188–200, Jan. 1999.

[63] M. Xing, R. Wu, J. Lan, and Z. Bao, "Migration through resolution cell compensation in ISAR imaging," *IEEE Geoscience and Remote Sensing Letters*, vol. 1, no. 2, pp. 141–144, Apr. 2004.

[64] D. Kirkland, "Imaging moving targets using the second-order keystone transform," *IET Radar, Sonar & Navigation*, vol. 5, no. 8, pp. 902–910, Oct. 2011.

[65] D. Li, M. Zhan, H. Liu, Y. Liao, and G. Liao, "A robust translational motion compensation method for ISAR imaging based on keystone transform and fractional Fourier transform under low SNR environment,"

IEEE Transactions on Aerospace and Electronic Systems, vol. 53, no. 5, pp. 2140–2156, Oct. 2017.

[66] G. Wang and Z. Bao, "The minimum entropy criterion of range alignment in ISAR motion compensation," in *Radar 97 (Conf. Publ. No. 449)*, Oct. 1997, pp. 236–239.

[67] L. Xi, L. Guosui, and J. Ni, "Autofocusing of ISAR images based on entropy minimization," *IEEE Transactions on Aerospace and Electronic Systems*, vol. 35, no. 4, pp. 1240–1252, Oct. 1999.

[68] M. Hu, L. Gao, and Z. Zhang, "A new ISAR range alignment method via minimum tsallis entropy," in *2013 IEEE International Conference on Microwave Technology Computational Electromagnetics*, Aug. 2013, pp. 391–394.

[69] J. Wang and D. Kasilingam, "Global range alignment for ISAR," *IEEE Transactions on Aerospace and Electronic Systems*, vol. 39, no. 1, pp. 351–357, Jan. 2003.

[70] J. Wang and X. Liu, "Improved global range alignment for ISAR," *IEEE Transactions on Aerospace and Electronic Systems*, vol. 43, no. 3, pp. 1070–1075, Jul. 2007.

[71] V. Janse van Rensburg, A. Mishra, and W. Nel, "Quality measures for HRR alignment based ISAR imaging algorithms," in *2013 IEEE Radar Conference*, May 2013, pp. 1–4.

[72] R. Vehmas and J. Jylhä, "Improving the estimation accuracy and computational efficiency of ISAR range alignment," in *2017 European Radar Conference (EURAD)*, Oct. 2017, pp. 13–16.

[73] R. Vehmas, J. Jylhä, M. Väilä, and J. Kylmälä, "A computationally feasible optimization approach to inverse SAR translational motion compensation," in *Proceedings of the12th European Radar Conference*, Sep. 2015, pp. 17–20.

[74] D. Zhu, L. Wang, Y. Yu, Q. Tao, and Z. Zhu, "Robust ISAR range alignment via minimizing the entropy of the average range profile," *IEEE Geoscience and Remote Sensing Letters*, vol. 6, no. 2, pp. 204–208, Apr. 2009.

[75] S.-B. Peng, J. Xu, Y.-N. Peng, and J.-B. Xiang, "Parametric inverse synthetic aperture radar manoeuvring target motion compensation based on particle swarm optimiser," *IET radar, sonar & navigation*, vol. 5, no. 3, pp. 305–314, Mar. 2011.

[76] Y. Li, T. Zhang, Z. Ding, W. Gao, and J. Chen, "An improved inverse synthetic aperture radar range alignment method based on maximum contrast," *The Journal of Engineering*, vol. 2019, no. 19, pp. 5467–5470, Oct. 2019.

[77] M. P. Hayes and P. T. Gough, "Synthetic aperture sonar: A review of current status," *IEEE Journal of Oceanic Engineering*, vol. 34, no. 3, pp. 207–224, Jul. 2009.

[78] B. Borden, "Maximum entropy regularization in inverse synthetic aperture radar imagery," *IEEE Transactions on Signal Processing*, vol. 40, no. 4, pp. 969–973, Apr. 1992.

[79] F. Berizzi and G. Corsini, "Autofocusing of inverse synthetic aperture radar images using contrast optimization," *IEEE Transactions on Aerospace and Electronic Systems*, vol. 32, no. 3, pp. 1185–1191, Jul. 1996.

[80] J. R. Fienup, "Synthetic aperture radar autofocus by maximizing sharpness," *Optics Letters*, vol. 25, no. 4, pp. 221–223, Feb. 2000.

[81] J. R. Fienup and J. J. Miller, "Aberration correction by maximizing generalized sharpness metrics," *The Journal of the Optical Society of America A*, vol. 20, no. 4, pp. 609–620, Apr. 2003.

[82] R. L. Morrison, M. N. Do, and D. C. Munson, "SAR image autofocus by sharpness optimization: a theoretical study," *IEEE Transactions on Image Processing*, vol. 16, no. 9, pp. 2309–2321, Sep. 2007.

[83] P. H. Eichel, D. C. Ghiglia, and C. V. Jakowatz, "Speckle processing method for synthetic-aperture-radar phase correction," *Optics Letters*, vol. 14, no. 1, pp. 1–3, Jan. 1989.

[84] D. E. Wahl, P. H. Eichel, D. C. Ghiglia, and C. V. Jakowatz, "Phase gradient autofocus - a robust tool for high resolution SAR phase correction," *IEEE Transactions on Aerospace and Electronic Systems*, vol. 30, no. 3, pp. 827–835, Jul. 1994.

[85] J. Cai, M. Martorella, S. Chang, Q. Liu, Z. Ding, and T. Long, "Efficient nonparametric ISAR autofocus algorithm based on contrast maximization and Newton's method," *IEEE Sensors Journal*, vol. 21, no. 4, pp. 4474–4487, Feb. 2021.

[86] P. T. Gough and R. G. Lane, "Autofocussing SAR and SAS images using a conjugate gradient search algorithm," in *Proceedings of IEEE International Geoscience and Remote Sensing Symposium (IGARSS)*, Seattle, WA, USA, Jul. 1998, pp. 621–623.

[87] S. A. Fortune, M. P. Hayes, and P. T. Gough, "Statistical autofocus of synthetic aperture sonar images using contrast optimization," in *Proceedings of IEEE International Geoscience and Remote Sensing Symposium (IGARSS)*, Sydney, Australia, Jul. 2001, pp. 1509–1511.

[88] F. Berizzi, M. Martorella, B. Haywood, E. D. Mese, and S. Bruscoli, "A survey on ISAR autofocusing techniques," in *Proceeding of the International Conference on Image Processing (ICIP)*, Oct. 2004, pp. 9–12.

[89] P. Cao, M. Xing, G. Sun, Y. Li, and Z. Bao, "Minimum entropy via subspace for ISAR autofocus," *IEEE Geoscience and Remote Sensing Letters*, vol. 7, no. 1, pp. 205–209, Jan. 2010.

[90] S. Zhang, Y. Liu, and X. Li, "Fast entropy minimization based autofocusing technique for ISAR imaging," *IEEE Transactions on Signal Processing*, vol. 63, no. 13, pp. 3425–3434, Jul. 2015.

[91] M. Kang, J. Bae, S. Lee, and K. Kim, "Efficient ISAR autofocus via minimization of Tsallis entropy," *IEEE Transactions on Aerospace and Electronic Systems*, vol. 52, no. 6, pp. 2950–2960, Dec. 2016.

[92] S. Lee, J. Bae, M. Kang, and K. Kim, "Efficient ISAR autofocus technique using eigenimages," *IEEE Journal of Selected Topics in Applied Earth Observations and Remote Sensing*, vol. 10, no. 2, pp. 605–616, Feb. 2017.

[93] D. Ligori, S. Wagner, L. Fabbrini, M. Greco, T. Bieker, G. Pinelli, and S. Brüggenwirth, "Nonparametric ISAR autofocusing via entropy- based Doppler centroid search," *IEEE Geoscience and Remote Sensing Letters*, vol. 15, no. 11, pp. 1725–1729, Nov. 2018.

[94] T. J. Schulz, "Optimal sharpness function for SAR autofocus," *IEEE Signal Processing Letters*, vol. 14, no. 1, pp. 27–30, Jan. 2007.

[95] J. Munoz-Ferreras, F. Perez-Martinez, and M. Datcu, "Generalisation of inverse synthetic aperture radar autofocusing methods based on the minimisation of the Renyi entropy," *IET Radar, Sonar & Navigation*, vol. 4, no. 4, pp. 586–594, Aug. 2010.

[96] J. Wang and X. Liu, "Measurement of sharpness and its application in ISAR imaging," *IEEE Transactions on Geoscience and Remote Sensing*, vol. 51, no. 9, pp. 4885–4892, Sep. 2013.

[97] H. L. Chan and T. S. Yeo, "Noniterative quality phase gradient autofocus (QPGA) algorithm for spotlight SAR imagery," *IEEE Transactions on Geoscience and Remote Sensing*, vol. 36, no. 5, pp. 1531–1539, Sep. 1998.

[98] W. Ye, T. S. Yeo, and Z. Bao, "Weighted least-squares estimation of phase errors for SAR/ISAR autofocus," *IEEE Transactions on Geoscience and Remote Sensing*, vol. 37, no. 5, pp. 2487–2494, Sep. 1999.

[99] S. A. Fortune, "Phase error estimation for synthetic aperture imagery," Ph.D. dissertation, University of Canterbury, Christchurch, New Zealand, 2005.

[100] P. Tsakalides and C. L. Nikias, "High-resolution autofocus techniques for SAR imaging based on fractional lower-order statistics," *IEE Proceedings on Radar, Sonar and Navigation*, vol. 148, no. 5, pp. 267–276, Oct. 2001.

[101] Z. She, D. A. Gray, and R. E. Bogner, "Autofocus for inverse synthetic aperture radar (ISAR) imaging," *Signal Processing*, vol. 81, no. 2, pp. 275–291, 2001.

[102] D. Zhu, R. Jiang, X. Mao, and Z. Zhu, "Multi-subaperture PGA for SAR autofocusing," *IEEE Transactions on Aerospace and Electronic Systems*, vol. 49, no. 1, pp. 468–488, Jan. 2013.

[103] J. Xu, J. Cai, Y. Sun, X. Xia, A. Farina, and T. Long, "Efficient ISAR phase autofocus based on eigenvalue decomposition," *IEEE Geoscience and Remote Sensing Letters*, vol. 14, no. 12, pp. 2195–2199, Dec. 2017.

[104] J. Rosebrock, G. D'Apice, S. Sommer, and D. Cerutti-Maori, "Modified phase gradient algorithm for ISAR image autofocus with large apertures," in *EUSAR 2018; 12th European Conference on Synthetic Aperture Radar*, Jun. 2018, pp. 1–6.

[105] R. Vehmas, "Computational algorithms for improved synthetic aperture radar image focusing," Ph.D. dissertation, Tampere University of Technology, Tampere, Finland, 2018.

[106] A. Evers and J. A. Jackson, "A generalized phase gradient autofocus algorithm," *IEEE Transactions on Computational Imaging*, vol. 5, no. 4, pp. 606–619, Dec. 2019.

[107] ——, "Generalized phase gradient autofocus using semidefinite relaxation phase estimation," *IEEE Transactions on Computational Imaging*, vol. 6, pp. 291–303, Oct. 2020.

[108] R. L. Morrison, M. N. Do, and D. C. Munson, "MCA: a multichannel approach to SAR autofocus," *IEEE Transactions on Image Processing*, vol. 18, no. 4, pp. 840–853, Apr. 2009.

[109] K.-H. Liu and D. C. Munson, "Fourier-domain multichannel autofocus for synthetic aperture radar," *IEEE Transactions on Image Processing*, vol. 20, no. 12, pp. 3544–3552, Dec. 2011.

[110] K.-H. Liu, A. Wiesel, and D. C. Munson, "Synthetic aperture radar autofocus via semidefinite relaxation," *IEEE Transactions on Image Processing*, vol. 22, no. 6, pp. 2317–2326, Jun. 2013.

[111] T. Itoh, H. Sueda, and Y. Watanabe, "Motion compensation for ISAR via centroid tracking," *IEEE Transactions on Aerospace and Electronic Systems*, vol. 32, no. 3, pp. 1191–1197, Jul. 1996.

[112] R. P. Bocker, T. B. Henderson, S. A. Jones, and B. R. Frieden, "New inverse synthetic aperture radar algorithm for translational motion compensation," in *Stochastic and Neural Methods in Signal Processing, Image Processing, and Computer Vision*, vol. 1569. International Society for Optics and Photonics, 1991, pp. 298–310.

[113] R. P. Bocker and S. A. Jones, "ISAR motion compensation using the burst derivative measure as a focal quality indicator," *International Journal of Imaging Systems and Technology*, vol. 4, no. 4, pp. 285–297, 1992.

[114] M. Martorella, F. Berizzi, and B. Haywood, "Contrast maximization based technique for 2-D ISAR autofocusing," *IEE Proceedings on Radar, Sonar and Navigation*, vol. 152, no. 4, pp. 253–262, Aug. 2005.

[115] L. Liu, F. Zhou, M. Tao, P. Sun, and Z. Zhang, "Adaptive translational motion compensation method for ISAR imaging under low SNR based on particle swarm optimization," *IEEE Journal of Selected Topics in Applied Earth Observations and Remote Sensing*, vol. 8, no. 11, pp. 5146–5157, Nov. 2015.

[116] G. Xu, M. Xing, L. Yang, and Z. Bao, "Joint approach of translational and rotational phase error corrections for high-resolution inverse synthetic aperture radar imaging using minimum-entropy," *IET Radar, Sonar & Navigation*, vol. 10, no. 3, pp. 586–594, Mar. 2016.

[117] S. Shao, L. Zhang, H. Liu, and Y. Zhou, "Accelerated translational motion compensation with contrast maximisation optimisation algorithm for inverse synthetic aperture radar imaging," *IET Radar, Sonar & Navigation*, vol. 13, no. 2, pp. 316–325, Feb. 2018.

[118] E. Yigit, "A translational motion compensation technique for inverse synthetic aperture radar images using multi-objective particle swarm optimization algorithm," *Microwave and Optical Technology Letters*, vol. 62, no. 6, pp. 2217–2225, 2020.

[119] D. Ustun and A. Toktas, "Translational motion compensation for ISAR images through a multicriteria decision using surrogate-based optimization," *IEEE Transactions on Geoscience and Remote Sensing*, vol. 58, no. 6, pp. 4365–4374, Jun. 2020.

[120] J. Li, R. Wu, and V. C. Chen, "Robust autofocus algorithm for ISAR imaging of moving targets," *IEEE Transactions on Aerospace and Electronic Systems*, vol. 37, no. 3, pp. 1056–1069, Jul. 2001.

[121] C. Noviello, G. Fornaro, P. Braca, and M. Martorella, "Fast and accurate ISAR focusing based on a Doppler parameter estimation algorithm," *IEEE Geoscience and Remote Sensing Letters*, vol. 14, no. 3, pp. 349–353, Mar. 2017.

[122] H. Fan, L. Ren, E. Mao, and Q. Liu, "A high-precision method of phase-derived velocity measurement and its application in motion compensation of ISAR imaging," *IEEE Transactions on Geoscience and Remote Sensing*, vol. 56, no. 1, pp. 60–77, Jan. 2018.

[123] G. Lu and Z. Bao, "Compensation of scatterer migration through resolution cell in inverse synthetic aperture radar imaging," *IEE Proceedings-Radar, Sonar and Navigation*, vol. 147, no. 2, pp. 80–85, Apr. 2000.

[124] M. Xing, R. Wu, and Z. Bao, "High resolution ISAR imaging of high speed moving targets," *IEE Proceedings on Radar, Sonar and Navigation*, vol. 152, no. 2, pp. 58–67, Apr. 2005.

[125] R. P. Perry, R. C. DiPietro, and R. L. Fante, "Coherent integration with range migration using keystone formatting," in *2007 IEEE Radar Conference*, Apr. 2007, pp. 863–868.

[126] D. Zhu, Y. Li, and Z. Zhu, "A keystone transform without interpolation for SAR ground moving-target imaging," *IEEE Geoscience and Remote Sensing Letters*, vol. 4, no. 1, pp. 18–22, Jan. 2007.

[127] K. Huo, Y. Liu, J. Hu, W. Jiang, and X. Li, "A novel imaging method for fast rotating targets based on the segmental pseudo keystone transform," *IEEE Transactions on Geoscience and Remote Sensing*, vol. 49, no. 4, pp. 1464–1472, Apr. 2011.

[128] Y. Li, M. Xing, J. Su, Y. Quan, and Z. Bao, "A new algorithm of ISAR imaging for maneuvering targets with low SNR," *IEEE Transactions on Aerospace and Electronic Systems*, vol. 49, no. 1, pp. 543–557, Jan. 2013.

[129] H. Ruan, Y. Wu, X. Jia, and W. Ye, "Novel ISAR imaging algorithm for maneuvering targets based on a modified keystone transform," *IEEE Geoscience and Remote Sensing Letters*, vol. 11, no. 1, pp. 128–132, Jan. 2014.

[130] R. Vehmas, J. Jylhä, M. Väilä, and A. Visa, "ISAR imaging of non-cooperative objects with non-uniform rotational motion," in *2016 IEEE Radar Conference (RadarConf)*, May 2016, pp. 932–937.

[131] V. C. Chen, "Reconstruction of inverse synthetic aperture radar image using adaptive time-frequency wavelet transform," in *SPIE's 1995 Symposium on OE/Aerospace Sensing and Dual Use Photonics*. International Society for Optics and Photonics, 1995, pp. 373–386.

[132] V. C. Chen and S. Qian, "Joint time-frequency transform for radar range-Doppler imaging," *IEEE Transactions on Aerospace and Electronic Systems*, vol. 34, no. 2, pp. 486–499, Apr. 1998.

[133] F. Berizzi, E. D. Mese, M. Diani, and M. Martorella, "High-resolution ISAR imaging of maneuvering targets by means of the range instantaneous Doppler technique: modeling and performance analysis," *IEEE Transactions on Image Processing*, vol. 10, no. 12, pp. 1880–1890, Dec. 2001.

[134] Z. Bao, C. Sun, and M. Xing, "Time-frequency approaches to ISAR imaging of maneuvering targets and their limitations," *IEEE Transactions on Aerospace and Electronic Systems*, vol. 37, no. 3, pp. 1091–1099, Jul. 2001.

[135] V. C. Chen and W. Miceli, "Time-varying spectral analysis for radar imaging of manoeuvring targets," *IEE Proceedings-Radar, Sonar and Navigation*, vol. 145, no. 5, pp. 262–268, Oct. 1998.

[136] X. Xia, G. Wang, and V. C. Chen, "Quantitative SNR analysis for ISAR imaging using joint time-frequency analysis - short time Fourier transform," *IEEE Transactions on Aerospace and Electronic Systems*, vol. 38, no. 2, pp. 649–659, Apr. 2002.

[137] J. M. Munoz-Ferreras and F. Perez-Martinez, "On the Doppler spreading effect for the range-instantaneous-Doppler technique in inverse synthetic aperture radar imagery," *IEEE Geoscience and Remote Sensing Letters*, vol. 7, no. 1, pp. 180–184, Jan. 2010.

[138] G. Wang, Z. Bao, and X. Sun, "Inverse synthetic aperture radar imaging of nonuniformly rotating targets," *Optical Engineering*, vol. 35, no. 10, pp. 3007–3011, 1996.

[139] Z. Bao, G. Wang, and L. Luo, "Inverse synthetic radar imaging of maneuvering targets," *Optical engineering*, vol. 37, no. 5, pp. 1582–1588, 1998.

[140] R. Wang and Y. C. Jiang, "ISAR ship imaging based on reassigned smoothed pseudo Wigner-Ville distribution," in *2010 International Conference on Multimedia Technology*, Oct. 2010, pp. 1–3.

[141] Y. Wang and Y. Jiang, "ISAR imaging of maneuvering target based on the L-class of fourth-order complex-lag PWVD," *IEEE Transactions on Geoscience and Remote Sensing*, vol. 48, no. 3, pp. 1518–1527, Mar. 2010.

[142] Y. Wang, J. Kang, and Y. Jiang, "ISAR imaging of maneuvering target based on the local polynomial Wigner distribution and integrated high-order ambiguity function for cubic phase signal model," *IEEE Journal of Selected Topics in Applied Earth Observations and Remote Sensing*, vol. 7, no. 7, pp. 2971–2991, Jul. 2014.

[143] S. Qian and D. Chen, "Signal representation using adaptive normalized gaussian functions," *Signal processing*, vol. 36, no. 1, pp. 1–11, 1994.

[144] L. C. Trintinalia and H. Ling, "Joint time-frequency ISAR using adaptive processing," *IEEE Transactions on Antennas and Propagation*, vol. 45, no. 2, pp. 221–227, Feb. 1997.

[145] Y. Wang, H. Ling, and V. C. Chen, "ISAR motion compensation via adaptive joint time-frequency technique," *IEEE Transactions on Aerospace and Electronic Systems*, vol. 34, no. 2, pp. 670–677, Apr. 1998.

[146] T. Thayaparan, G. Lampropoulos, S. K. Wong, and E. Riseborough, "Application of adaptive joint time-frequency algorithm for focusing distorted ISAR images from simulated and measured radar data," *IEE Proceedings on Radar, Sonar and Navigation*, vol. 150, no. 4, pp. 213–220, Aug. 2003.

[147] T. Thayaparan, W. Brinkman, and G. Lampropoulos, "Inverse synthetic aperture radar image focusing using fast adaptive joint time–frequency and three-dimensional motion detection on experimental radar data," *IET Signal Processing*, vol. 4, no. 4, pp. 382–394, Aug. 2010.

[148] W. Brinkman and T. Thayaparan, "Focusing inverse synthetic aperture radar images with higher-order motion error using the adaptive joint-time–frequency algorithm optimised with the genetic algorithm and the particle swarm optimisation algorithm–comparison and results," *IET Signal Processing*, vol. 4, no. 4, pp. 329–342, Aug. 2010.

[149] L. Stankovic, "A method for time-frequency analysis," *IEEE Transactions on Signal Processing*, vol. 42, no. 1, pp. 225–229, Jan. 1994.

[150] L. J. Stankovic, T. Thayaparan, M. Dakovic, and V. Popovic, "S-method in radar imaging," in *Proceedings of the14th European Signal Processing Conference*, Sep. 2006, pp. 1–5.

[151] L. J. Stankovic, T. Thayaparan, V. Popovic, I. Djurovic, and M. Dakovic, "Adaptive S-method for SAR/ISAR imaging," *EURASIP Journal on Advances in Signal Processing*, vol. 2008, pp. 1–10, 2008.

[152] T. Thayaparan, L. J. Stankovic, C. Wernik, and M. Dakovic, "Real-time motion compensation, image formation and image enhancement of moving targets in ISAR and SAR using s-method-based approach," *IET Signal Processing*, vol. 2, no. 3, pp. 247–264, Sep. 2008.

[153] S. Stankovic, I. Orovic, and A. Krylov, "Two-dimensional hermite S-method for high-resolution inverse synthetic aperture radar imaging applications," *IET Signal Processing*, vol. 4, no. 4, pp. 352–362, Aug. 2010.

[154] L. Du and G. Su, "Adaptive inverse synthetic aperture radar imaging for nonuniformly moving targets," *IEEE Geoscience and Remote Sensing Letters*, vol. 2, no. 3, pp. 247–249, Jul. 2005.

[155] I. Djurović, T. Thayaparan, and L. Stanković, "Adaptive local polynomial Fourier transform in ISAR," *EURASIP Journal on Applied Signal Processing*, vol. 2006, pp. 129–129, 2006.

[156] I. Daubechies, J. Lu, and H.-T. Wu, "Synchrosqueezed wavelet transforms: An empirical mode decomposition-like tool," *Applied and computational harmonic analysis*, vol. 30, no. 2, pp. 243–261, 2011.

[157] F. Auger and P. Flandrin, "Improving the readability of time-frequency and time-scale representations by the reassignment method," *IEEE Transactions on Signal Processing*, vol. 43, no. 5, pp. 1068–1089, May 1995.

[158] P. Suresh, T. Thayaparan, and K. Venkataramaniah, "ISAR imaging of moving targets based on reassigned smoothed pseudo Wigner-Ville distribution," in *Proceedings of International Radar Symposium India, IRSI-2011*, 2011.

[159] D. Li, H. Liu, X. Gui, and X. Zhang, "An efficient ISAR imaging method for maneuvering target based on synchrosqueezing transform," *IEEE Antennas and Wireless Propagation Letters*, vol. 15, pp. 1317–1320, Dec. 2016.

[160] G. Wang and Z. Bao, "Inverse synthetic aperture radar imaging of maneuvering targets based on chirplet decomposition," *Optical Engineering*, vol. 38, no. 9, pp. 1534–1541, 1999.

[161] L. Wu, X. Wei, D. Yang, H. Wang, and X. Li, "ISAR imaging of targets with complex motion based on discrete chirp Fourier transform for cubic chirps," *IEEE Transactions on Geoscience and Remote Sensing*, vol. 50, no. 10, pp. 4201–4212, Oct. 2012.

[162] Y. Wang and Y. Jiang, "Approach for high-resolution inverse synthetic aperture radar imaging of ship target with complex motion," *IET Signal Processing*, vol. 7, no. 2, pp. 146–157, Apr. 2013.

[163] Y. Wang, B. Zhao, and Y. Jiang, "Inverse synthetic aperture radar imaging of targets with complex motion based on cubic chirplet decomposition," *IET Signal Processing*, vol. 9, no. 5, pp. 419–429, Jul. 2015.

[164] Y. Li, R. Wu, M. Xing, and Z. Bao, "Inverse synthetic aperture radar imaging of ship target with complex motion," *IET Radar, Sonar & Navigation*, vol. 2, no. 6, pp. 395–403, Dec. 2008.

[165] Y. Wang and Y. Jiang, "ISAR imaging of a ship target using product high-order matched-phase transform," *IEEE Geoscience and Remote Sensing Letters*, vol. 6, no. 4, pp. 658–661, Oct. 2009.

[166] X. Lv, M. Xing, C. Wan, and S. Zhang, "ISAR imaging of maneuvering targets based on the range centroid Doppler technique," *IEEE Transactions on Image Processing*, vol. 19, no. 1, pp. 141–153, Jan. 2010.

[167] Y. Wang and Y. Jiang, "Inverse synthetic aperture radar imaging of maneuvering target based on the product generalized cubic phase function," *IEEE Geoscience and Remote Sensing Letters*, vol. 8, no. 5, pp. 958–962, Sep. 2011.

[168] Y. Wang and Y. Jiang, "Inverse synthetic aperture radar imaging of three-dimensional rotation target based on two-order match Fourier transform," *IET Signal Processing*, vol. 6, no. 2, pp. 159–169, Apr. 2012.

[169] Y. Wang, "Inverse synthetic aperture radar imaging of manoeuvring target based on range-instantaneous-Doppler and range-instantaneous-chirp-rate algorithms," *IET Radar, Sonar & Navigation*, vol. 6, no. 9, pp. 921–928, Dec. 2012.

[170] C. Wang, Y. Wang, and S. Li, "Inverse synthetic aperture radar imaging of ship targets with complex motion based on match Fourier transform for cubic chirps model," *IET Radar, Sonar & Navigation*, vol. 7, no. 9, pp. 994–1003, Dec. 2013.

[171] X. Bai, R. Tao, Z. Wang, and Y. Wang, "ISAR imaging of a ship target based on parameter estimation of multicomponent quadratic frequency-modulated signals," *IEEE Transactions on Geoscience and Remote Sensing*, vol. 52, no. 2, pp. 1418–1429, Feb. 2014.

[172] Y. Wang and Y. Lin, "ISAR imaging of non-uniformly rotating target via range-instantaneous-Doppler-derivatives algorithm," *IEEE Journal of Selected Topics in Applied Earth Observations and Remote Sensing*, vol. 7, no. 1, pp. 167–176, Jan. 2014.

[173] J. Zheng, T. Su, L. Zhang, W. Zhu, and Q. H. Liu, "ISAR imaging of targets with complex motion based on the chirp rate–quadratic chirp rate distribution," *IEEE Transactions on Geoscience and Remote Sensing*, vol. 52, no. 11, pp. 7276–7289, Nov. 2014.

[174] J. Zheng, T. Su, W. Zhu, and Q. H. Liu, "ISAR imaging of targets with complex motions based on the keystone time-chirp rate distribution," *IEEE Geoscience and Remote Sensing Letters*, vol. 11, no. 7, pp. 1275–1279, Jul. 2014.

[175] Y. Wang and B. Zhao, "Inverse synthetic aperture radar imaging of nonuniformly rotating target based on the parameters estimation of multicomponent quadratic frequency-modulated signals," *IEEE Sensors Journal*, vol. 15, no. 7, pp. 4053–4061, Jul. 2015.

[176] J. Zheng, T. Su, G. Liao, H. Liu, Z. Liu, and Q. H. Liu, "ISAR imaging for fluctuating ships based on a fast bilinear parameter estimation algorithm," *IEEE Journal of Selected Topics in Applied Earth Observations and Remote Sensing*, vol. 8, no. 8, pp. 3954–3966, Aug. 2015.

[177] Y. Li, T. Su, J. Zheng, and X. He, "ISAR imaging of targets with complex motions based on modified Lv's distribution for cubic phase signal," *IEEE Journal of Selected Topics in Applied Earth Observations and Remote Sensing*, vol. 8, no. 10, pp. 4775–4784, Oct. 2015.

[178] J. Zheng, T. Su, W. Zhu, L. Zhang, Z. Liu, and Q. H. Liu, "ISAR imaging of nonuniformly rotating target based on a fast parameter estimation algorithm of cubic phase signal," *IEEE Transactions on Geoscience and Remote Sensing*, vol. 53, no. 9, pp. 4727–4740, Sep. 2015.

[179] D. Li, X. Gui, H. Liu, J. Su, and H. Xiong, "An ISAR imaging algorithm for maneuvering targets with low SNR based on parameter estimation of multicomponent quadratic FM signals and nonuniform FFT," *IEEE Journal of Selected Topics in Applied Earth Observations and Remote Sensing*, vol. 9, no. 12, pp. 5688–5702, Dec. 2016.

[180] Q. Lv, T. Su, and J. Zheng, "Inverse synthetic aperture radar imaging of targets with complex motion based on the local polynomial ambiguity function," *Journal of Applied Remote Sensing*, vol. 10, no. 1, p. 015019, 2016.

[181] J. Zheng, H. Liu, G. Liao, T. Su, Z. Liu, and Q. H. Liu, "ISAR imaging of targets with complex motions based on a noise-resistant parameter estimation algorithm without nonuniform axis," *IEEE Sensors Journal*, vol. 16, no. 8, pp. 2509–2518, Apr. 2016.

[182] ——, "ISAR imaging of nonuniformly rotating targets based on generalized decoupling technique," *IEEE Journal of Selected Topics in Applied Earth Observations and Remote Sensing*, vol. 9, no. 1, pp. 520–532, Jan. 2016.

[183] Y. Wang, R. Xu, Q. Zhang, and B. Zhao, "ISAR imaging of maneuvering target based on the quadratic frequency modulated signal model with time-varying amplitude," *IEEE Journal of Selected Topics in Applied Earth Observations and Remote Sensing*, vol. 10, no. 3, pp. 1012–1024, Mar. 2017.

[184] D. Li, M. Zhan, X. Zhang, Z. Fang, and H. Liu, "ISAR imaging of nonuniformly rotating target based on the multicomponent CPS model under low SNR environment," *IEEE Transactions on Aerospace and Electronic Systems*, vol. 53, no. 3, pp. 1119–1135, Jun. 2017.

[185] L. Zuo and B. Wang, "ISAR imaging of non-uniform rotating targets based on optimized matching Fourier transform," *IEEE Access*, vol. 8, pp. 64 324–64 330, Mar. 2020.

[186] X. Bai, M. Xing, F. Zhou, and Z. Bao, "High-resolution three-dimensional imaging of spinning space debris," *IEEE Transactions on Geoscience and Remote Sensing*, vol. 47, no. 7, pp. 2352–2362, Jul. 2009.

[187] J. X. Lopez and Z. Qiao, "Filtered back projection inversion of turntable ISAR data," in *Proc. SPIE*, vol. 8051, 2011, pp. 80 510 901–80 510 909.

[188] T. Ray, Y. Cao, Z. Qiao, and G. Chen, "2D and 3D ISAR image reconstruction through filtered back projection," in *Radar Sensor Technology XVI*, vol. 8361. International Society for Optics and Photonics, 2012, p. 836107.

[189] J. Jylhä, M. Väilä, H. Perälä, V. Väisänen, A. Visa, R. Vehmas, J. Kylmälä, and V. Salminen, "On SAR processing using pixel-wise matched kernels," in *2014 11th European Radar Conference*, Oct. 2014, pp. 97–100.

[190] I. Pisciottano, F. Santi, D. Pastina, and D. Cristallini, "DVB-S based passive polarimetric ISAR—methods and experimental validation," *IEEE Sensors Journal*, vol. 21, no. 5, pp. 6056–6070, Mar. 2021.

[191] R. Vehmas and J. Jylhä, "A contrast optimization algorithm for back-projection image reconstruction in noncooperative ISAR imaging," in *EUSAR 2018; 12th European Conference on Synthetic Aperture Radar*, Jun. 2018, pp. 1–6.

[192] A. Sommer and J. Ostermann, "Backprojection subimage autofocus of moving ships for synthetic aperture radar," *IEEE Transactions on Geoscience and Remote Sensing*, vol. 57, no. 11, pp. 8383–8393, Nov. 2019.

[193] Z.-S. Liu, R. Wu, and J. Li, "Complex ISAR imaging of maneuvering targets via the Capon estimator," *IEEE Transactions on Signal Processing*, vol. 47, no. 5, pp. 1262–1271, May 1999.

[194] A. D. Lazarov, "Iterative MMSE method and recurrent Kalman procedure for isar image reconstruction," *IEEE Transactions on Aerospace and Electronic Systems*, vol. 37, no. 4, pp. 1432–1441, Oct. 2001.

[195] P. Hu, S. Xu, W. Wu, B. Tian, and Z. Chen, "IAA-based high-resolution ISAR imaging with small rotational angle," *IEEE Geoscience and Remote Sensing Letters*, vol. 14, no. 11, pp. 1978–1982, Nov. 2017.

[196] S. G. Qadir and Y. Fan, "Two-dimensional superresolution inverse synthetic aperture radar imaging using hybridized SVSV algorithm," *IEEE Transactions on Antennas and Propagation*, vol. 61, no. 2, pp. 1012–1015, Feb. 2013.

[197] M. Martorella and F. Berizzi, "Time windowing for highly focused ISAR image reconstruction," *IEEE Transactions on Aerospace and Electronic Systems*, vol. 41, no. 3, pp. 992–1007, Jul. 2005.

[198] D. Pastina and C. Spina, "Slope-based frame selection and scaling technique for ship ISAR imaging," *IET Signal Processing*, vol. 2, no. 3, pp. 265–276, Sep. 2008.

[199] A. W. Rihaczek and S. J. Hershkowitz, "Choosing imaging intervals for small ships," in *Radar Processing, Technology, and Applications IV*, vol. 3810. International Society for Optics and Photonics, 1999, pp. 139–148.

[200] D. Pastina, A. Montanari, and A. Aprile, "Motion estimation and optimum time selection for ship ISAR imaging," in *Proceedings of the 2003 IEEE Radar Conference (Cat. No. 03CH37474)*, May 2003, pp. 7–14.

[201] M. Y. Abdul Gaffar, W. A. J. Nel, and M. R. Inggs, "Selecting suitable coherent processing time window lengths for ground-based ISAR imaging of cooperative sea vessels," *IEEE Transactions on Geoscience and Remote Sensing*, vol. 47, no. 9, pp. 3231–3240, Sep. 2009.

[202] F. Berizzi, M. Martorella, and E. Giusti, *Radar imaging for maritime observation*. CRC Press, 2018.

[203] P. Zhou, X. Zhang, W. Sun, Y. Dai, and Y. Wan, "Time-frequency analysis-based time-windowing algorithm for the inverse synthetic aperture radar imaging of ships," *Journal of Applied Remote Sensing*, vol. 12, no. 1, p. 015001, 2018.

[204] B. Kang, B. Ryu, C. Kim, and K. Kim, "Improved frame-selection scheme for ISAR imaging of targets in complex 3-D motion," *IEEE Sensors Journal*, vol. 18, no. 1, pp. 111–121, Jan. 2018.

[205] P. Zhou, X. Zhang, Y. Dai, W. Sun, and Y. Wan, "Time window selection algorithm for ISAR ship imaging based on instantaneous Doppler frequency estimations of multiple scatterers," *IEEE Journal of Selected Topics in Applied Earth Observations and Remote Sensing*, vol. 12, no. 10, pp. 3799–3812, Oct. 2019.

[206] J. Wang, L. Zhang, L. Du, B. Chen, and H. Liu, "Optimal coherent processing interval selection for aerial maneuvering target imaging using tracking information," *IEEE Sensors Journal*, vol. 18, no. 10, pp. 4117–4128, May 2018.

[207] F. Prodi, "ISAR cross-range scaling using a correlation based functional," in *IEEE RADAR 2008*, May 2008, pp. 1–6.

[208] Y. Wang and Y. Jiang, "A novel algorithm for estimating the rotation angle in ISAR imaging," *IEEE Geoscience and Remote Sensing Letters*, vol. 5, no. 4, pp. 608–609, Oct. 2008.

[209] W. Li, X. Wang, and G. Wang, "Scaled Radon-Wigner transform imaging and scaling of maneuvering target," *IEEE Transactions on Aerospace and Electronic Systems*, vol. 46, no. 4, pp. 2043–2051, Oct. 2010.

[210] C.-M. Yeh, J.Yang, Y.-N. Peng, and X.-M. Shan, "Rotation estimation for ISAR targets with a space-time analysis technique," *IEEE Geoscience and Remote Sensing Letters*, vol. 8, no. 5, pp. 899–903, Sep. 2011.

[211] S.-B. Peng, J. Xu, Y.-N. Peng, J.-B. Xiang, and X.-G. Xia, "Inverse synthetic aperture radar rotation velocity estimation based on phase slope difference of two prominent scatterers," *IET Radar, Sonar & Navigation*, vol. 5, no. 9, pp. 1002–1009, Dec. 2011.

[212] N. Li and L. Wang, "A new cross-range scaling method for ISAR based on the multiple dominant scatterers synthesis," in *Proceedings of 2011 IEEE CIE International Conference on Radar*, vol. 1. IEEE, Oct. 2011, pp. 666–669.

[213] L. Liu, F. Zhou, M.-l. Tao, B. Zhao, and Z.-j. Zhang, "Cross-range scaling method of inverse synthetic aperture radar image based on discrete polynomial-phase transform," *IET Radar, Sonar & Navigation*, vol. 9, no. 3, pp. 333–341, Mar. 2014.

[214] Y. Du, Y. Jiang, and W. Zhou, "An accurate two-step ISAR cross-range scaling method for earth-orbit target," *IEEE Geoscience and Remote Sensing Letters*, vol. 14, no. 11, pp. 1893–1897, Nov. 2017.

[215] Y. Wang, X. Huang, and R. Cao, "Novel method of ISAR cross-range scaling for slowly rotating targets based on the iterative adaptive approach and discrete polynomial-phase transform," *IEEE Sensors Journal*, vol. 19, no. 13, pp. 4898–4906, Jul. 2019.

[216] Y. Gao, M. Xing, Z. Zhang, and L. Guo, "ISAR imaging and cross-range scaling for maneuvering targets by using the NCS-NLS algorithm," *IEEE Sensors Journal*, vol. 19, no. 13, pp. 4889–4897, Jul. 2019.

[217] S. Sibo, Z. Xinyu, Z. Guangpu, L. Guolong, and Z. Chunhui, "Accurate ISAR scaling for both smooth and maneuvering targets," *IEEE Transactions on Aerospace and Electronic Systems*, vol. 55, no. 3, pp. 1537–1549, Jun. 2019.

[218] Y. Wang, X. Huang, and R. Cao, "Novel approach for ISAR cross-range scaling based on the multidelay discrete polynomial- phase transform combined with keystone transform," *IEEE Transactions on Geoscience and Remote Sensing*, vol. 58, no. 2, pp. 1221–1231, Feb. 2020.

[219] Y. Wang, X. Huang, and Q. Zhang, "Rotation parameters estimation and cross-range scaling research for range instantaneous Doppler ISAR images," *IEEE Sensors Journal*, vol. 20, no. 13, pp. 7010–7020, Jul. 2020.

[220] C.-M. Yeh, J. Xu, Y.-N. Peng, and X.-T. Wang, "Cross-range scaling for ISAR based on image rotation correlation," *IEEE Geoscience and Remote Sensing Letters*, vol. 6, no. 3, pp. 597–601, Jul. 2009.

[221] S.-H. Park, H.-T. Kim, and K.-T. Kim, "Cross-range scaling algorithm for ISAR images using 2-D Fourier transform and polar mapping," *IEEE Transactions on Geoscience and Remote Sensing*, vol. 49, no. 2, pp. 868–877, Feb. 2011.

[222] Z. Xu, L. Zhang, and M. Xing, "Precise cross-range scaling for ISAR images using feature registration," *IEEE Geoscience and Remote Sensing Letters*, vol. 11, no. 10, pp. 1792–1796, Oct. 2014.

[223] X. Wang, M. Zhang, and J. Zhao, "Efficient cross-range scaling method via two-dimensional unitary ESPRIT scattering center extraction algorithm," *IEEE Geoscience and Remote Sensing Letters*, vol. 12, no. 5, pp. 928–932, May 2015.

[224] F.-L. Su and H.-X. Yang, "Cross-range scaling technique for ISAR images with affine projection matrix," *Electronics Letters*, vol. 52, no. 14, pp. 1255–1257, Jul. 2016.

[225] M. Kang, J. Bae, B. Kang, and K. Kim, "ISAR cross-range scaling using iterative processing via principal component analysis and bisection algorithm," *IEEE Transactions on Signal Processing*, vol. 64, no. 15, pp. 3909–3918, Aug. 2016.

[226] B. Kang, J. Bae, M. Kang, E. Yang, and K. Kim, "ISAR cross-range scaling via joint estimation of rotation center and velocity," *IEEE Transactions on Aerospace and Electronic Systems*, vol. 52, no. 4, pp. 2023–2029, Aug. 2016.

[227] S. Jeong, B. Kang, M. Kang, and K. Kim, "ISAR cross-range scaling using Radon transform and its projection," *IEEE Transactions on Aerospace and Electronic Systems*, vol. 54, no. 5, pp. 2590–2600, Oct. 2018.

[228] D. Li, C. Zhang, H. Liu, J. Su, X. Tan, Q. Liu, and G. Liao, "A fast cross-range scaling algorithm for ISAR images based on the 2-D discrete wavelet transform and pseudopolar fourier transform," *IEEE Transactions on Geoscience and Remote Sensing*, vol. 57, no. 7, pp. 4231–4245, Jul. 2019.

[229] F. E. McFadden, "Three-dimensional reconstruction from ISAR sequences," in *Radar Sensor Technology and Data Visualization*, vol. 4744. International Society for Optics and Photonics, 2002, pp. 58–67.

[230] L. Liu, F. Zhou, X. Bai, M. Tao, and Z. Zhang, "Joint cross-range scaling and 3D geometry reconstruction of ISAR targets based on factorization method," *IEEE Transactions on Image Processing*, vol. 25, no. 4, pp. 1740–1750, Apr. 2016.

[231] C. Zhou, L. Jiang, Q. Yang, X. Ren, and Z. Wang, "High precision cross-range scaling and 3D geometry reconstruction of ISAR targets based on geometrical analysis," *IEEE Access*, vol. 8, pp. 132 415–132 423, 2020.

[232] D. Pastina, "Rotation motion estimation for high resolution ISAR and hybrid SAR/ISAR target imaging," in *2008 IEEE Radar Conference*, May 2008, pp. 1–6.

[233] J. Sheng, M. Xing, L. Zhang, M. Q. Mehmood, and L. Yang, "ISAR cross-range scaling by using sharpness maximization," *IEEE Geoscience and Remote Sensing Letters*, vol. 12, no. 1, pp. 165–169, Jan. 2015.

[234] S. Zhang, Y. Liu, X. Li, and G. Bi, "Fast ISAR cross-range scaling using modified Newton method," *IEEE Transactions on Aerospace and Electronic Systems*, vol. 54, no. 3, pp. 1355–1367, Jun. 2018.

[235] S. Brisken, "Multistatic ISAR - chances and challenges," in *Radar Conference (Radar), 2014 International*, Oct. 2014, pp. 1–6.

[236] Z. Zhu, Y. Zhang, and Z. Tang, "Bistatic inverse synthetic aperture radar imaging," in *IEEE International Radar Conference, 2005.* IEEE, 2005, pp. 354–358.

[237] M. Martorella, J. Palmer, J. Homer, B. Littleton, and I. D. Longstaff, "On bistatic inverse synthetic aperture radar," *IEEE Transactions on Aerospace and Electronic Systems*, vol. 43, no. 3, pp. 1125–1134, Jul. 2007.

[238] V. C. Chen, A. des Rosiers, and R. Lipps, "Bi-static ISAR range-doppler imaging and resolution analysis," in *2009 IEEE Radar Conference*, May 2009, pp. 1–5.

[239] S. Zhang, S. Sun, W. Zhang, Z. Zong, and T. Soon Yeo, "High-resolution bistatic ISAR image formation for high-speed and complex-motion targets," *IEEE Journal of Selected Topics in Applied Earth Observations and Remote Sensing*, vol. 8, no. 7, pp. 3520–3531, Jul. 2015.

[240] Z. Liu and Y. Jiang, "A novel Doppler frequency model and imaging procedure analysis for bistatic ISAR configuration with shorebase transmitter and shipborne receiver," *IEEE Journal of Selected Topics in Applied Earth Observations and Remote Sensing*, vol. 9, no. 7, pp. 2989–3000, Jul. 2016.

[241] Y. Jiang, S. Sun, T. S. Yeo, and Y. Yuan, "Bistatic ISAR distortion and defocusing analysis," *IEEE Transactions on Aerospace and Electronic Systems*, vol. 52, no. 3, pp. 1168–1182, Jun. 2016.

[242] M. Kang, B. Kang, S. Lee, and K. Kim, "Bistatic-ISAR distortion correction and range and cross-range scaling," *IEEE Sensors Journal*, vol. 17, no. 16, pp. 5068–5078, Aug. 2017.

[243] B. Kang, J. Bae, M. Kang, E. Yang, and K. Kim, "Bistatic-ISAR cross-range scaling," *IEEE Transactions on Aerospace and Electronic Systems*, vol. 53, no. 4, pp. 1962–1973, Aug. 2017.

[244] D. Cataldo and M. Martorella, "Bistatic isar distortion mitigation via superresolution," *IEEE Transactions on Aerospace and Electronic Systems*, vol. 54, no. 5, pp. 2143–2157, Oct. 2018.

[245] D. Pastina, M. Bucciarelli, and P. Lombardo, "Multi-platform distributed ISAR for surveillance and recognition," in *2009 International Radar Conference" Surveillance for a Safer World"(RADAR 2009).* IEEE, Oct. 2009, pp. 1–6.

[246] D. Pastina, M. Bucciarelli, and P. Lombardo, "Multistatic and MIMO distributed ISAR for enhanced cross-range resolution of rotating targets," *IEEE Transactions on Geoscience and Remote Sensing*, vol. 48, no. 8, pp. 3300–3317, Aug. 2010.

[247] L. Wang, M. Cheney, and B. Borden, "Multistatic radar imaging of moving targets," *IEEE Transactions on Aerospace and Electronic Systems*, vol. 48, no. 1, pp. 230–242, Jan. 2012.

[248] P. Van Dorp, M. P. G. Otten, and J. M. M. Verzeilberg, "Coherent multistatic ISAR imaging," in *IET International Conference on Radar Systems (Radar 2012).* IET, Oct. 2012, pp. 1–6.

[249] S. Brisken, D. Matthes, T. Mathy, and J. G. Worms, "Spatially diverse ISAR imaging for classification performance enhancement," *International Journal of Electronics and Telecommunications*, vol. 57, pp. 15–22, 2011.

[250] S. Brisken and J. G. Worms, "ISAR motion parameter estimation via multilateration," in *2011 Microwaves, Radar and Remote Sensing Symposium*, Aug. 2011, pp. 190–194.

[251] S. Brisken and M. Martorella, "Multistatic ISAR autofocus with an image entropy-based technique," *IEEE Aerospace and Electronic Systems Magazine*, vol. 29, no. 7, pp. 30–36, Jul. 2014.

[252] S. Brisken and J. Ender, "Block-sparse 3-D ISAR image reconstruction in a non-coherent multistatic scenario," in *2015 IEEE Radar Conference (RadarCon)*, May 2015, pp. 0265–0269.

[253] S. Brisken, "Motion estimation and imaging with multistatic inverse synthetic aperture radar," Ph.D. dissertation, University of Siegen, Siegen, Germany, 2016.

[254] M. Cetin and A. D. Lanterman, "Region-enhanced passive radar imaging," *IEE Proceedings-Radar, Sonar and Navigation*, vol. 152, no. 3, pp. 185–194, Jun. 2005.

[255] J. Garry, C. Baker, G. Smith, and R. Ewing, "Doppler imaging for passive bistatic radar," in *2013 IEEE Radar Conference (RadarCon13).* IEEE, May 2013, pp. 1–6.

[256] S. Wacks and B. Yazıcı, "Passive synthetic aperture hitchhiker imaging of ground moving targets—Part 1: Image formation and velocity estimation," *IEEE Transactions on Image Processing*, vol. 23, no. 6, pp. 2487–2500, Jun. 2014.

[257] K. Suwa, S. Nakamura, S. Morita, T. Wakayama, H. Maniwa, T. Oshima, R. Maekawa, S. Matsuda, and T. Tachihara, "ISAR imaging of an aircraft target using ISDB-T digital TV based passive bistatic radar," in *2010 IEEE International Geoscience and Remote Sensing Symposium*, Jul. 2010, pp. 4103–4105.

[258] P. Krysik, K. Kulpa, P. Samczynski, K. Szumski, and J. Misiurewicz, "Moving target detection and imaging using GSM-based passive radar," in *IET International Conference on Radar Systems (Radar 2012)*, Oct. 2012, pp. 1–4.

[259] D. Olivadese, E. Giusti, D. Petri, M. Martorella, A. Capria, F. Berizzi, and R. Soleti, "Passive isar imaging of ships by using dvb-t signals," in *IET International Conference on Radar Systems (Radar 2012)*, Oct. 2012, pp. 1–4.

[260] D. Olivadese, E. Giusti, D. Petri, M. Martorella, A. Capria, and F. Berizzi, "Passive ISAR with DVB-T signals," *IEEE Transactions on Geoscience and Remote Sensing*, vol. 51, no. 8, pp. 4508–4517, Aug. 2013.

[261] M. K. Baczyk, P. Samczynski, and K. Kulpa, "Passive ISAR imaging of air targets using DVB-T signals," in *2014 IEEE Radar Conference*, May 2014, pp. 0502–0506.

[262] L. Wang and B. Yazici, "Passive imaging of moving targets using sparse distributed apertures," *SIAM Journal on Imaging Sciences*, vol. 5, no. 3, pp. 769–808, Jul. 2012.

[263] M. Martorella and E. Giusti, "Theoretical foundation of passive bistatic ISAR imaging," *IEEE Transactions on Aerospace and Electronic Systems*, vol. 50, no. 3, pp. 1647–1659, Jul. 2014.

[264] J. L. Garry and G. E. Smith, "Passive ISAR part I: framework and considerations," *IET Radar, Sonar & Navigation*, vol. 13, no. 2, pp. 169–180, Feb. 2019.

[265] ——, "Passive ISAR part II: narrowband imaging," *IET Radar, Sonar & Navigation*, vol. 13, no. 2, pp. 181–189, Feb. 2019.

[266] F. Colone, D. Pastina, P. Falcone, and P. Lombardo, "WiFi-based passive ISAR for high-resolution cross-range profiling of moving targets," *IEEE Transactions on Geoscience and Remote Sensing*, vol. 52, no. 6, pp. 3486–3501, Jun. 2014.

[267] F. Colone, D. Pastina, and V. Marongiu, "VHF cross-range profiling of aerial targets via passive ISAR: Signal processing schemes and experimental results," *IEEE Transactions on Aerospace and Electronic Systems*, vol. 53, no. 1, pp. 218–235, Feb. 2017.

[268] J. L. Garry, G. E. Smith, and C. J. Baker, "Wideband DTV passive ISAR system design," in *2015 IEEE Radar Conference (RadarCon)*, May 2015, pp. 0834–0839.

[269] P. Samczynski, K. Kulpa, M. K. Baczyk, and D. Gromek, "SAR/ISAR imaging in passive radars," in *2016 IEEE Radar Conference (RadarConf)*, May 2016, pp. 1–6.

[270] S. Brisken, M. Moscadelli, V. Seidel, and C. Schwark, "Passive radar imaging using DVB-S2," in *2017 IEEE Radar Conference (RadarConf)*, May 2017, pp. 0552–0556.

[271] I. Pisciottano, D. Pastina, and D. Cristallini, "DVB-S based passive radar imaging of ship targets," in *2019 20th International Radar Symposium (IRS)*, Jun. 2019, pp. 1–7.

[272] I. Pisciottano, D. Cristallini, and D. Pastina, "Maritime target imaging via simultaneous DVB-T and DVB-S passive ISAR," *IET Radar, Sonar & Navigation*, vol. 13, no. 9, pp. 1479–1487, Sep. 2019.

[273] I. Pisciottano, D. Cristallini, D. Pastina, and F. Santi, "Experimental results of polarimetric passive ISAR exploiting DVB-S2 illumination," in *2020 IEEE International Radar Conference (RADAR)*, Apr. 2020, pp. 518–523.

[274] F. Santi, F. Pieralice, D. Pastina, M. Antoniou, and M. Cherniakov, "Passive radar imagery of ship targets by using navigation satellites transmitters of opportunity," in *2019 20th International Radar Symposium (IRS)*, Jun. 2019, pp. 1–10.

[275] F. Santi, D. Pastina, M. Antoniou, and M. Cherniakov, "GNSS-based multistatic passive radar imaging of ship targets," in *2020 IEEE International Radar Conference (RADAR)*, Apr. 2020, pp. 601–606.

[276] D. Pastina, F. Santi, F. Pieralice, M. Antoniou, and M. Cherniakov, "Passive radar imaging of ship targets with GNSS signals of opportunity," *IEEE Transactions on Geoscience and Remote Sensing*, vol. 59, no. 3, pp. 2627–2642, Mar. 2021.

[277] M. Soumekh, "Automatic aircraft landing using interferometric inverse synthetic aperture radar imaging," *IEEE Transactions on Image Processing*, vol. 5, no. 9, pp. 1335–1345, Sep. 1996.

[278] X. Xu, H. Luo, and P. Huang, "3-D interferometric ISAR images for scattering diagnosis of complex radar targets," in *Proceedings of the 1999 IEEE Radar Conference. Radar into the Next Millennium (Cat. No.99CH36249)*, Apr. 1999, pp. 237–241.

[279] G. Wang, X.-G. Xia, and V. C. Chen, "Three-dimensional ISAR imaging of maneuvering targets using three receivers," *IEEE Transactions on Image Processing*, vol. 10, no. 3, pp. 436–447, Mar. 2001.

[280] X. Xu and R. M. Narayanan, "Three-dimensional interferometric ISAR imaging for target scattering diagnosis and modeling," *IEEE Transactions on Image Processing*, vol. 10, no. 7, pp. 1094–1102, Jul. 2001.

[281] Q. Zhang and T. S. Yeo, "Three-dimensional SAR imaging of a ground moving target using the InISAR technique," *IEEE Transactions on Geoscience and Remote Sensing*, vol. 42, no. 9, pp. 1818–1828, Sep. 2004.

[282] J. A. Given and W. R. Schmidt, "Generalized ISAR - part I: an optimal method for imaging large naval vessels," *IEEE Transactions on Image Processing*, vol. 14, no. 11, pp. 1783–1791, Nov. 2005.

[283] ——, "Generalized ISAR-part II: interferometric techniques for three-dimensional location of scatterers," *IEEE Transactions on Image Processing*, vol. 14, no. 11, pp. 1792–1797, Nov. 2005.

[284] C. Ma, T. S. Yeo, Q. Zhang, H. S. Tan, and J. Wang, "Three-dimensional ISAR imaging based on antenna array," *IEEE Transactions on Geoscience and Remote Sensing*, vol. 46, no. 2, pp. 504–515, Feb. 2008.

[285] C. Ma, T. S. Yeo, H. S. Tan, J. Wang, and B. Chen, "Three-dimensional ISAR imaging using a two-dimensional sparse antenna array," *IEEE Geoscience and Remote Sensing Letters*, vol. 5, no. 3, pp. 378–382, Jul. 2008.

[286] Y. Liu, M. Song, K. Wu, R. Wang, and Y. Deng, "High-quality 3-D InISAR imaging of maneuvering target based on a combined processing approach," *IEEE Geoscience and Remote Sensing Letters*, vol. 10, no. 5, pp. 1036–1040, Sep. 2013.

[287] M. Martorella, F. Salvetti, and D. Staglianò, "3D target reconstruction by means of 2D-ISAR imaging and interferometry," in *2013 IEEE Radar Conference (RadarCon13)*, May 2013, pp. 1–6.

[288] M. Martorella, D. Staglianò, F. Salvetti, and N. Battisti, "3D interferometric ISAR imaging of noncooperative targets," *IEEE Transactions on Aerospace and Electronic Systems*, vol. 50, no. 4, pp. 3102–3114, Oct. 2014.

[289] D. Staglianò, M. Martorella, and E. Casalini, "Interferometric bistatic ISAR processing for 3D target reconstruction," in *2014 11th European Radar Conference*, Oct. 2014, pp. 161–164.

[290] L. Zhao, M. Gao, M. Martorella, and D. Staglianò, "Bistatic three-dimensional interferometric ISAR image reconstruction," *IEEE Transactions on Aerospace and Electronic Systems*, vol. 51, no. 2, pp. 951–961, Apr. 2015.

[291] Q. Lv, T. Su, J. Zheng, and J. Zhang, "Three-dimensional interferometric inverse synthetic aperture radar imaging of maneuvering target based on the joint cross modified Wigner-Ville distribution," *Journal of Applied Remote Sensing*, vol. 10, no. 1, p. 015007, 2016.

[292] A. Fontana, P. Berens, D. Staglianò, and M. Martorella, "3D ISAR/SAR imaging using multichannel real data," in *2016 IEEE Radar Conference (RadarConf)*, May 2016, pp. 1–4.

[293] Y. Wang and X. Li, "Three-dimensional interferometric ISAR imaging for the ship target under the bi-static configuration," *IEEE Journal of Selected Topics in Applied Earth Observations and Remote Sensing*, vol. 9, no. 4, pp. 1505–1520, Apr. 2016.

[294] Y. Wang and X. Chen, "3-D interferometric inverse synthetic aperture radar imaging of ship target with complex motion," *IEEE Transactions on Geoscience and Remote Sensing*, vol. 56, no. 7, pp. 3693–3708, Jul. 2018.

[295] M. Nasirian and M. H. Bastani, "A novel model for three-dimensional imaging using interferometric ISAR in any curved target flight path," *IEEE Transactions on Geoscience and Remote Sensing*, vol. 52, no. 6, pp. 3236–3245, Jun. 2014.

[296] D. Felguera-Martín, J.-T. González-Partida, P. Almorox-González, M. Burgos-García, and B.-P. Dorta-Naranjo, "Interferometric inverse synthetic aperture radar experiment using an interferometric linear frequency modulated continuous wave millimetre-wave radar," *IET Radar, Sonar & Navigation*, vol. 5, no. 1, pp. 39–47, Jan. 2011.

[297] E. Giusti and M. Martorella, "Passive 3D interferometric ISAR using target-borne illuminator of opportunity," *IET Radar, Sonar & Navigation*, vol. 13, no. 2, pp. 190–197, Feb. 2019.

[298] F. Salvetti, D. Staglianò, E. Giusti, and M. Martorella, "Multistatic 3D ISAR image reconstruction," in *2015 IEEE Radar Conference (RadarCon)*, May 2015, pp. 0640–0645.

[299] F. Salvetti, E. Giusti, D. Staglianò, and M. Martorella, "Incoherent fusion of 3D InISAR images using multi-temporal and multi-static data," in *2016 IEEE Radar Conference (RadarConf)*. IEEE, May 2016, pp. 1–6.

[300] F. Salvetti, M. Martorella, E. Giusti, and D. Staglianò, "Multiview three-dimensional interferometric inverse synthetic aperture radar," *IEEE Transactions on Aerospace and Electronic Systems*, vol. 55, no. 2, pp. 718–733, Apr. 2019.

[301] Q. Zhang, T. S. Yeo, G. Du, and S. Zhang, "Estimation of three-dimensional motion parameters in interferometric ISAR imaging," *IEEE Transactions on Geoscience and Remote Sensing*, vol. 42, no. 2, pp. 292–300, Feb. 2004.

[302] M. Martorella, J. Palmero, F. Berizzi, and E. Dalle Mese, "Improving the total rotation vector estimation via a bistatic ISAR system," in *Proceedings. 2005 IEEE International Geoscience and Remote Sensing Symposium, 2005. IGARSS'05.*, vol. 2. IEEE, Jul. 2005, pp. 1068–1071.

[303] F. Santi, D. Pastina, and M. Bucciarelli, "Multi-sensor ISAR techniques for motion estimation of pitching, rolling and yawing targets," in *2013 IEEE Radar Conference (RadarCon13)*. IEEE, Apr. 2013, pp. 1–6.

[304] H.-T. Tran, E. Giusti, M. Martorella, F. Salvetti, B. W.-H. Ng, and A. Phan, "Estimation of the total rotational velocity of a non-cooperative target using a 3D InISAR system," in *2015 IEEE Radar Conference (RadarCon)*. IEEE, May 2015, pp. 0937–0941.

[305] B. W.-H. Ng, H.-T. Tran, M. Martorella, E. Giusti, F. Salvetti, and A. Phan, "Estimation of the total rotational velocity of a non-cooperative target with a high cross-range resolution three-dimensional interferometric inverse synthetic aperture radar system," *IET Radar, Sonar & Navigation*, vol. 11, no. 6, pp. 1020–1029, Jun. 2017.

[306] F. Santi, D. Pastina, and M. Bucciarelli, "Estimation of ship dynamics with a multiplatform radar imaging system," *IEEE Transactions on Aerospace and Electronic Systems*, vol. 53, no. 6, pp. 2769–2788, Dec. 2017.

[307] J. R. Fienup, "Detecting moving targets in SAR imagery by focusing," *IEEE Transactions on Aerospace and Electronic Systems*, vol. 37, no. 3, pp. 794–809, Jul. 2001.

[308] F. Zhou, R. Wu, M. Xing, and Z. Bao, "Approach for single channel SAR ground moving target imaging and motion parameter estimation," *IET Radar, Sonar and Navigation*, vol. 1, no. 1, pp. 59–66, Feb. 2007.

[309] D. Zhu, Y. Li, and Z. Zhu, "A keystone transform without interpolation for SAR ground moving-target imaging," *IEEE Geoscience and Remote Sensing Letters*, vol. 4, no. 1, pp. 18–22, Jan. 2007.

[310] S. Zhu, G. Liao, Y. Qu, Z. Zhou, and X. Liu, "Ground moving targets imaging algorithm for synthetic aperture radar," *IEEE Transactions on Geoscience and Remote Sensing*, vol. 49, no. 1, pp. 462–477, Jan. 2011.

[311] M. Martorella, E. Giusti, F. Berizzi, A. Bacci, and E. D. Mese, "ISAR based techniques for refocusing non-cooperative targets in SAR images," *IET Radar, Sonar and Navigation*, vol. 6, no. 5, pp. 332–340, Jun. 2012.

[312] M. Martorella, D. Pastina, F. Berizzi, and P. Lombardo, "Spaceborne radar imaging of maritime moving targets with the Cosmo-SkyMed SAR system," *IEEE Journal of Selected Topics in Applied Earth Observations and Remote Sensing*, vol. 7, no. 7, pp. 2797–2810, Jul. 2014.

[313] C. Noviello, G. Fornaro, and M. Martorella, "Focused SAR image formation of moving targets based on Doppler parameters estimation," *IEEE Transactions on Geoscience and Remote Sensing*, vol. 53, no. 6, pp. 3460–3470, Jun. 2015.

[314] T. K. Sjögren, V. T. Vu, M. I. Pettersson, A. Gustavsson, and L. M. H. Ulander, "Moving target relative speed estimation and refocusing in synthetic aperture radar images," *IEEE Transactions on Aerospace and Electronic Systems*, vol. 48, no. 3, pp. 2426–2436, Jul. 2012.

[315] V. T. Vu, M. I. Pettersson, and T. K. Sjögren, "Moving target focusing in SAR image with known normalized relative speed," *IEEE Transactions on Aerospace and Electronic Systems*, vol. 53, no. 2, pp. 854–861, Apr. 2017.

[316] J. Ward, "Space-time adaptive processing for airborne radar," Massachusetts Institue of Technology, Lincoln Laboratory, Tech. Rep. 1015, 1994.

[317] A. Bacci, D. Gray, M. Martorella, and F. Berizzi, "Joint STAP-ISAR for non-cooperative target imaging in strong clutter," in *2013 IEEE Radar Conference (RadarCon13)*, May 2013, pp. 1–5.

[318] T. K. Sjögren, V. T. Vu, M. I. Pettersson, F. Wang, D. J. G. Murdin, A. Gustavsson, and L. M. H. Ulander, "Suppression of clutter in multichannel SAR GMTI," *IEEE Transactions on Geoscience and Remote Sensing*, vol. 52, no. 7, pp. 4005–4013, Jul. 2013.

[319] S.-X. Zhang, M.-D. Xing, X.-G. Xia, R. Guo, Y.-Y. Liu, and Z. Bao, "Robust clutter suppression and moving target imaging approach for multichannel in azimuth high-resolution and wide-swath synthetic aperture radar," *IEEE Transactions on Geoscience and Remote Sensing*, vol. 53, no. 2, pp. 687–709, Feb. 2014.

[320] A. Bacci, "Optimal space time adaptive processing for multichannel inverse synthetic aperture radar imaging," Ph.D. dissertation, University of Adelaide, Adelaide, Australia, 2014.

[321] A. Bacci, M. Martorella, D. A. Gray, and F. Berizzi, "Space-Doppler adaptive processing for radar imaging of moving targets masked by ground clutter," *IET Radar, Sonar & Navigation*, vol. 9, no. 6, pp. 712–726, Jul. 2015.

[322] S. Gelli, A. Bacci, M. Martorella, and F. Berizzi, "Clutter suppression and high-resolution imaging of noncooperative ground targets for bistatic airborne radar," *IEEE Transactions on Aerospace and Electronic Systems*, vol. 54, no. 2, pp. 932–949, Apr. 2018.

[323] A. Bacci, M. Martorella, D. A. Gray, S. Gelli, and F. Berizzi, "Virtual multichannel SAR for ground moving target imaging," *IET Radar, Sonar & Navigation*, vol. 10, no. 1, pp. 50–62, Jan. 2016.

[324] L. Stankovic, I. Djurovic, and T. Thayaparan, "Separation of target rigid body and micro-doppler effects in isar imaging," *IEEE Transactions on Aerospace and Electronic Systems*, vol. 42, no. 4, pp. 1496–1506, Oct. 2006.

[325] L. Stankovic, T. Thayaparan, M. Dakovic, and V. Popovic-Bugarin, "Micro-Doppler removal in the radar imaging analysis," *IEEE Transactions on Aerospace and Electronic Systems*, vol. 49, no. 2, pp. 1234–1250, Apr. 2013.

[326] L. Stanković, S. Stanković, T. Thayaparan, M. Daković, and I. Orović, "Separation and reconstruction of the rigid body and micro-Doppler signal in ISAR part I–theory," *IET Radar, Sonar & Navigation*, vol. 9, no. 9, pp. 1147–1154, Dec. 2015.

[327] ——, "Separation and reconstruction of the rigid body and micro-Doppler signal in ISAR part II–statistical analysis," *IET Radar, Sonar & Navigation*, vol. 9, no. 9, pp. 1155–1161, Dec. 2015.

[328] Y. Wang, X. Zhou, and R. Zhang, "Removal of micro-Doppler effect in ISAR imaging based on time recursive iterative adaptive approach," *IET Radar, Sonar & Navigation*, vol. 14, no. 8, pp. 1159–1166, Aug. 2020.

[329] Q. Zhang, T. S. Yeo, H. S. Tan, and Y. Luo, "Imaging of a moving target with rotating parts based on the hough transform," *IEEE Transactions on Geoscience and Remote Sensing*, vol. 46, no. 1, pp. 291–299, Jan. 2008.

[330] Y. Luo, Q. Zhang, C.-w. Qiu, X.-j. Liang, and K.-m. Li, "Micro-Doppler effect analysis and feature extraction in ISAR imaging with stepped-frequency chirp signals," *IEEE Transactions on Geoscience and Remote Sensing*, vol. 48, no. 4, pp. 2087–2098, Apr. 2010.

[331] X. Bai, F. Zhou, M. Xing, and Z. Bao, "High resolution ISAR imaging of targets with rotating parts," *IEEE Transactions on Aerospace and Electronic Systems*, vol. 47, no. 4, pp. 2530–2543, Oct. 2011.

[332] W. Zhou, C.-m. Yeh, R.-j. Jin, Z.-h. Li, S.-l. Song, and J. Yang, "ISAR imaging of targets with rotating parts based on robust principal component analysis," *IET Radar, Sonar & Navigation*, vol. 11, no. 4, pp. 563–569, Apr. 2017.

[333] X. Bai, M. Xing, F. Zhou, G. Lu, and Z. Bao, "Imaging of micromotion targets with rotating parts based on empirical-mode decomposition," *IEEE Transactions on Geoscience and Remote Sensing*, vol. 46, no. 11, pp. 3514–3523, Nov. 2008.

[334] B. Yuan, Z. Chen, and S. Xu, "Micro-Doppler analysis and separation based on complex local mean decomposition for aircraft with fast-rotating parts in ISAR imaging," *IEEE Transactions on Geoscience and Remote Sensing*, vol. 52, no. 2, pp. 1285–1298, Feb. 2014.

[335] W. Kang, Y. Zhang, and X. Dong, "Micro-Doppler effect removal for ISAR imaging based on bivariate variational mode decomposition," *IET Radar, Sonar & Navigation*, vol. 12, no. 1, pp. 74–81, Jan. 2018.

[336] M. G. Czerwinski and J. M. Usoff, "Development of the haystack ultra-wideband satellite imaging radar," *Lincoln laboratory journal*, vol. 21, no. 1, pp. 28–44, 2014.

[337] D. Mehrholz, "Radar observations in low earth orbit," *Advances in Space Research*, vol. 19, no. 2, pp. 203–212, 1997.

[338] J. Ender, L. Leushacke, A. Brenner, and H. Wilden, "Radar techniques for space situational awareness," in *2011 12th International Radar Symposium (IRS)*, Sep. 2011, pp. 21–26.

[339] S. Sommer, V. Karamanavis, F. Schlichthaber, T. Patzelt, J. Rosebrock, D. Cerutti-Maori, and L. Leushacke, "Analysis of the attitude motion and cross-sectional area of Tiangong-1 during its uncontrolled re-entry," in *Proceedings of the 1st NEO and Debris Detection Conference*. ESA Space Safety Programme Office Darmstadt, Germany, 2019.

[340] S. Anger, M. Jirousek, S. Dill, and M. Peichl, "Research on advanced space surveillance using the IoSiS radar system," in *EUSAR 2021; 13th European Conference on Synthetic Aperture Radar*, Mar. 2021, pp. 1–4.

[341] L. C. Potter, E. Ertin, J. T. Parker, and M. Cetin, "Sparsity and compressed sensing in radar imaging," *Proceedings of the IEEE*, vol. 98, no. 6, pp. 1006–1020, Jun. 2010.

[342] M. Çetin, I. Stojanović, N. . Önhon, K. Varshney, S. Samadi, W. C. Karl, and A. S. Willsky, "Sparsity-driven synthetic aperture radar imaging: Reconstruction, autofocusing, moving targets, and compressed sensing," *IEEE Signal Processing Magazine*, vol. 31, no. 4, pp. 27–40, Jul. 2014.

[343] L. Zhang, M. Xing, C. Qiu, J. Li, and Z. Bao, "Achieving higher resolution ISAR imaging with limited pulses via compressed sampling," *IEEE Geoscience and Remote Sensing Letters*, vol. 6, no. 3, pp. 567–571, Jul. 2009.

[344] L. Zhang, Z. Qiao, M. Xing, J. Sheng, R. Guo, and Z. Bao, "High-resolution ISAR imaging by exploiting sparse apertures," *IEEE Transactions on Antennas and Propagation*, vol. 60, no. 2, pp. 997–1008, Feb. 2012.

[345] G. Xu, M. Xing, L. Zhang, J. Duan, Q. Chen, and Z. Bao, "Sparse apertures ISAR imaging and scaling for maneuvering targets," *IEEE Journal of Selected Topics in Applied Earth Observations and Remote Sensing*, vol. 7, no. 7, pp. 2942–2956, Jul. 2014.

[346] L. Zhang, J. Duan, Z. Qiao, M. Xing, and Z. Bao, "Phase adjustment and isar imaging of maneuvering targets with sparse apertures," *IEEE Transactions on Aerospace and Electronic Systems*, vol. 50, no. 3, pp. 1955–1973, Jul. 2014.

[347] G. Xu, M. Xing, and Z. Bao, "High-resolution inverse synthetic aperture radar imaging of manoeuvring targets with sparse aperture," *Electronics Letters*, vol. 51, no. 3, pp. 287–289, Feb. 2015.

[348] Q. Chen, G. Xu, L. Zhang, M. Xing, and Z. Bao, "Three-dimensional interferometric inverse synthetic aperture radar imaging with limited pulses by exploiting joint sparsity," *IET Radar, Sonar & Navigation*, vol. 9, no. 6, pp. 692–701, Jul. 2015.

[349] S. Tomei, A. Bacci, E. Giusti, M. Martorella, and F. Berizzi, "Compressive sensing-based inverse synthetic radar imaging imaging from incomplete data," *IET Radar, Sonar & Navigation*, vol. 10, no. 2, pp. 386–397, Feb. 2016.

[350] J. Bae, B. Kang, S. Lee, E. Yang, and K. Kim, "Bistatic ISAR image reconstruction using sparse-recovery interpolation of missing data," *IEEE Transactions on Aerospace and Electronic Systems*, vol. 52, no. 3, pp. 1155–1167, Jun. 2016.

[351] G. Xu, L. Yang, G. Bi, and M. Xing, "Maneuvering target imaging and scaling by using sparse inverse synthetic aperture," *Signal Processing*, vol. 137, pp. 149–159, 2017.

[352] A. S. Khwaja and X. Zhang, "Compressed sensing ISAR reconstruction in the presence of rotational acceleration," *IEEE Journal of Selected Topics in Applied Earth Observations and Remote Sensing*, vol. 7, no. 7, pp. 2957–2970, Jul. 2014.

[353] D.-r. Huang, L. Zhang, M.-D. Xing, G. Xu, J. Duan, and Z. Bao, "Sparse aperture inverse synthetic aperture radar imaging of manoeuvring targets with compensation of migration through range cells," *IET Radar, Sonar & Navigation*, vol. 8, no. 9, pp. 1164–1176, Dec. 2014.

[354] X. He, N. Tong, and X. Hu, "High-resolution imaging and 3-D reconstruction of precession targets by exploiting sparse apertures," *IEEE Transactions on Aerospace and Electronic Systems*, vol. 53, no. 3, pp. 1212–1220, Jun. 2017.

[355] L. Zhang, Z. Qiao, M. Xing, Y. Li, and Z. Bao, "High-resolution ISAR imaging with sparse stepped-frequency waveforms," *IEEE Transactions on Geoscience and Remote Sensing*, vol. 49, no. 11, pp. 4630–4651, Nov. 2011.

[356] H. Wang, Y. Quan, M. Xing, and S. Zhang, "ISAR imaging via sparse probing frequencies," *IEEE Geoscience and Remote Sensing Letters*, vol. 8, no. 3, pp. 451–455, May 2011.

[357] M. Kang, S. Lee, S. Lee, and K. Kim, "ISAR imaging of high-speed maneuvering target using gapped stepped-frequency waveform and com-

pressive sensing," *IEEE Transactions on Image Processing*, vol. 26, no. 10, pp. 5043–5056, Oct. 2017.

[358] A. Bacci, D. Staglianó, E. Giusti, S. Tomei, F. Berizzi, and M. Martorella, "Compressive sensing for interferometric inverse synthetic aperture radar applications," *IET Radar, Sonar & Navigation*, vol. 10, no. 8, pp. 1446–1457, Oct. 2016.

[359] J. Yang, "High-resolution multiple-input–multiple-output–inverse synthetic aperture radar imaging based on sparse representation," *IET Radar, Sonar & Navigation*, vol. 10, pp. 1277–1285(8), Aug. 2016.

[360] W. Qiu, M. Martorella, J. Zhou, H. Zhao, and Q. Fu, "Three-dimensional inverse synthetic aperture radar imaging based on compressive sensing," *IET Radar, Sonar & Navigation*, vol. 9, no. 4, pp. 411–420, Apr. 2015.

[361] J. Rong, Y. Wang, and T. Han, "Iterative optimization-based ISAR imaging with sparse aperture and its application in interferometric ISAR imaging," *IEEE Sensors Journal*, vol. 19, no. 19, pp. 8681–8693, Oct. 2019.

[362] F. Wang, F. Xu, and Y. Jin, "Three-dimensional reconstruction from a multiview sequence of sparse ISAR imaging of a space target," *IEEE Transactions on Geoscience and Remote Sensing*, vol. 56, no. 2, pp. 611–620, Feb. 2018.

[363] Y. Liu, N. Li, R. Wang, and Y. Deng, "Achieving high-quality three-dimensional InISAR imageries of maneuvering target via super-resolution ISAR imaging by exploiting sparseness," *IEEE Geoscience and Remote Sensing Letters*, vol. 11, no. 4, pp. 828–832, Apr. 2014.

[364] G. Xu, M. Xing, X. Xia, L. Zhang, Q. Chen, and Z. Bao, "3D geometry and motion estimations of maneuvering targets for interferometric ISAR with sparse aperture," *IEEE Transactions on Image Processing*, vol. 25, no. 5, pp. 2005–2020, May 2016.

[365] E. Giusti, D. Cataldo, A. Bacci, S. Tomei, and M. Martorella, "ISAR image resolution enhancement: Compressive sensing versus state-of-the-art super-resolution techniques," *IEEE Transactions on Aerospace and Electronic Systems*, vol. 54, no. 4, pp. 1983–1997, Aug. 2018.

[366] G. Xu, M. Xing, L. Zhang, Y. Liu, and Y. Li, "Bayesian inverse synthetic aperture radar imaging," *IEEE Geoscience and Remote Sensing Letters*, vol. 8, no. 6, pp. 1150–1154, Nov. 2011.

[367] H. Liu, B. Jiu, H. Liu, and Z. Bao, "Superresolution ISAR imaging based on sparse bayesian learning," *IEEE Transactions on Geoscience and Remote Sensing*, vol. 52, no. 8, pp. 5005–5013, Aug. 2014.

[368] Y. Wu, S. Zhang, H. Kang, and T. S. Yeo, "Fast marginalized sparse bayesian learning for 3-D interferometric ISAR image formation via super-resolution ISAR imaging," *IEEE Journal of Selected Topics in Applied Earth Observations and Remote Sensing*, vol. 8, no. 10, pp. 4942–4951, Oct. 2015.

[369] H. Duan, L. Zhang, J. Fang, L. Huang, and H. Li, "Pattern-coupled sparse bayesian learning for inverse synthetic aperture radar imaging," *IEEE Signal Processing Letters*, vol. 22, no. 11, pp. 1995–1999, Nov. 2015.

[370] G. Xu, L. Yang, G. Bi, and M. Xing, "Enhanced ISAR imaging and motion estimation with parametric and dynamic sparse Bayesian learning," *IEEE Transactions on Computational Imaging*, vol. 3, no. 4, pp. 940–952, Dec. 2017.

[371] R. Entezari and A. Rashidi, "Continuity pattern-based sparse Bayesian learning for inverse synthetic aperture radar imaging," *Journal of Applied Remote Sensing*, vol. 12, no. 3, p. 036010, 2018.

[372] S. Zhang, Y. Liu, and X. Li, "Bayesian bistatic ISAR imaging for targets with complex motion under low SNR condition," *IEEE Transactions on Image Processing*, vol. 27, no. 5, pp. 2447–2460, May 2018.

[373] H. Kang, J. Li, Q. Guo, and M. Martorella, "Pattern coupled sparse Bayesian learning based on UTAMP for robust high resolution ISAR imaging," *IEEE Sensors Journal*, vol. 20, no. 22, pp. 13 734–13 742, Nov. 2020.

[374] Y. Wang and Q. Liu, "Super-resolution sparse aperture ISAR imaging of maneuvering target via the RELAX algorithm," *IEEE Sensors Journal*, vol. 18, no. 21, pp. 8726–8738, Nov. 2018.

[375] G. Li, H. Zhang, X. Wang, and X. Xia, "ISAR 2-D imaging of uniformly rotating targets via matching pursuit," *IEEE Transactions on Aerospace and Electronic Systems*, vol. 48, no. 2, pp. 1838–1846, Apr. 2012.

[376] B. Jiu, H. Liu, H. Liu, L. Zhang, Y. Cong, and Z. Bao, "Joint ISAR imaging and cross-range scaling method based on compressive sensing with adaptive dictionary," *IEEE Transactions on Antennas and Propagation*, vol. 63, no. 5, pp. 2112–2121, May 2015.

[377] C. Hu, L. Wang, and O. Loffeld, "Inverse synthetic aperture radar imaging exploiting dictionary learning," in *2018 IEEE Radar Conference (RadarConf18)*, Apr. 2018, pp. 1084–1088.

[378] S. Zhang, Y. Liu, and X. Li, "Autofocusing for sparse aperture ISAR imaging based on joint constraint of sparsity and minimum entropy," *IEEE Journal of Selected Topics in Applied Earth Observations and Remote Sensing*, vol. 10, no. 3, pp. 998–1011, Mar. 2017.

[379] X. Du, C. Duan, and W. Hu, "Sparse representation based autofocusing technique for ISAR images," *IEEE Transactions on Geoscience and Remote Sensing*, vol. 51, no. 3, pp. 1826–1835, Mar. 2013.

[380] L. Zhao, L. Wang, G. Bi, and L. Yang, "An autofocus technique for high-resolution inverse synthetic aperture radar imagery," *IEEE Transactions on Geoscience and Remote Sensing*, vol. 52, no. 10, pp. 6392–6403, Oct. 2014.

[381] D. Xiao, F. Su, and J. Gao, "Autofocus approach for sparse aperture inverse synthetic aperture radar imaging," *Electronics Letters*, vol. 51, no. 22, pp. 1811–1813, Oct. 2015.

[382] H. R. Hashempour and M. A. Masnadi-Shirazi, "Inverse synthetic aperture radar phase adjustment and cross-range scaling based on sparsity," *Digital Signal Processing*, vol. 68, pp. 93–101, 2017.

[383] M. Kang, S. Lee, K. Kim, and J. Bae, "Bistatic ISAR imaging and scaling of highly maneuvering target with complex motion via compressive sensing," *IEEE Transactions on Aerospace and Electronic Systems*, vol. 54, no. 6, pp. 2809–2826, Dec. 2018.

[384] S. Zhang, Y. Liu, X. Li, and G. Bi, "Joint sparse aperture ISAR autofocusing and scaling via modified Newton method-based variational bayesian inference," *IEEE Transactions on Geoscience and Remote Sensing*, vol. 57, no. 7, pp. 4857–4869, Jul. 2019.

[385] S. Shao, L. Zhang, and H. Liu, "High-resolution ISAR imaging and motion compensation with 2-D joint sparse reconstruction," *IEEE Transactions on Geoscience and Remote Sensing*, vol. 58, no. 10, pp. 6791–6811, Oct. 2020.

[386] K. El-Darymli, E. W. Gill, P. Mcguire, D. Power, and C. Moloney, "Automatic target recognition in synthetic aperture radar imagery: A state-of-the-art review," *IEEE Access*, vol. 4, pp. 6014–6058, 2016.

[387] C. Y. Hu, L. Wang, Z. Li, L. Sun, and O. Loffeld, "Inverse synthetic aperture radar imaging using complex-value deep neural network," *The Journal of Engineering*, vol. 2019, no. 20, pp. 7096–7099, 2019.

[388] J. Gao, B. Deng, Y. Qin, H. Wang, and X. Li, "Enhanced radar imaging using a complex-valued convolutional neural network," *IEEE Geoscience and Remote Sensing Letters*, vol. 16, no. 1, pp. 35–39, Jan. 2019.

[389] C. Hu, L. Wang, Z. Li, and D. Zhu, "Inverse synthetic aperture radar imaging using a fully convolutional neural network," *IEEE Geoscience and Remote Sensing Letters*, vol. 17, no. 7, pp. 1203–1207, Jul. 2020.

[390] R. Li, S. Zhang, C. Zhang, Y. Liu, and X. Li, "Deep learning approach for sparse aperture ISAR imaging and autofocusing based on complex-valued ADMM-net," *IEEE Sensors Journal*, vol. 21, no. 3, pp. 3437–3451, Feb. 2021.

[391] X. Gao, D. Qin, and J. Gao, "Resolution enhancement for inverse synthetic aperture radar images using a deep residual network," *Microwave and Optical Technology Letters*, vol. 62, no. 4, pp. 1588–1593, 2020.

[392] D. Qin and X. Gao, "Enhancing ISAR resolution by a generative adversarial network," *IEEE Geoscience and Remote Sensing Letters*, vol. 18, no. 1, pp. 127–131, Jan. 2021.

[393] H. Mu, Y. Zhang, C. Ding, Y. Jiang, M. H. Er, and A. C. Kot, "DeepImaging: A ground moving target imaging based on CNN for SAR-GMTI system," *IEEE Geoscience and Remote Sensing Letters*, vol. 18, no. 1, pp. 117–121, Jan. 2021.

This article has been accepted for publication in a future issue of this journal, but has not been fully edited. Content may change prior to final publication. Citation information: DOI 10.1109/ACCESS.2021.3104799, IEEE Access

RISTO VEHMAS received his M.Sc. degree in theoretical physics from the University of Oulu, Oulu, Finland, in 2014, and his Ph.D. degree in computing and electrical engineering from the Tampere University of Technology, Tampere, Finland, in 2018. From 2019 to 2020, he was with Fraunhofer FHR in Wachtberg, Germany, where his research focused on signal processing algorithms for array-based radar systems. Currently, he is with Elettronica GmbH, Meckenheim, Germany, where he works as a System Analyst. His current research interests include analysis and modeling of radar systems in electronic warfare applications.

NADAV NEUBERGER received the B.Sc. degree in electrical and computer engineering from Ben-Gurion University, Beer Sheva, Israel in 2012, and the M.Sc. degree in electrical and electronic engineering from Tel Aviv University, Tel Aviv, Israel, in 2017. He is currently working towards the completion of a Ph.D. degree in electrical engineering in Siegen University, Siegen, Germany.

After completing the B.Sc. degree, he worked as an Electrical Engineer in the private sector in large companies and small scale start-ups. His major research areas were electromagnetics and human vital signs monitoring through radar. Since 2018 he works for Fraunhofer FHR, Germany. His current focus is on phased array radar signal processing for improved space situational awareness.